Z'-boson dilepton searches and the high-*x* quark density

J. Fiaschi, F. Giuli, F. Hautmann, S. Moch, S. Moretti

Phys.Lett.B 841 (2023) 137915

Precision era at the LHC

The forthcoming LHC Run-III will provide unique opportunities:

- Proton collisions at unprecedented 13.6 TeV energy will probe higher scales where we hope to observe signals of **BSM** physics.
- Opens the era of precision measurements at the LHC with very high statistics to accurately test **SM** predictions.

In this picture, a precise determination of the PDFs becomes crucial, as in many cases represents the dominant source of uncertainties.

In particular ***Z'/W'*** searches require a precise knowledge of **quark and anti-quark PDFs** in the high-x region, in order to probe the multi-TeV regime.

Recently there has been a fervent discussions on the subject:

A. Courtoy, P. Nadolsky (2021)
A. Courtoy, P. Nadolsky (2022)

where also the importance of the A_{FB} observable has been stressed:

R. D. Ball, et al. (2022)
M. Xie, et al. (2022)

Furthermore, the large-scale gluon PDF also receives sizeable contributions from the quark PDFs during the QCD evolution in the singlet sector due to the splitting function P_{gq}.
The large-x/large-scale gluon PDF benefits from an accurate determination of large-x quark PDFs.

S. Alekhin, et al. (2017)

Constraining quark PDFs

Light flavour separation has been traditionally studied using charged-lepton DIS data on proton and deuterium targets (additional complication from describing the deuterons as nucleon bound states).

Combination of DIS data and W-asymmetry measurements at Tevatron indicates $d_v/u_v \to 0$ for $x \to 1$.

S. Alekin, S. A. Kulagin, R. Petti (2017)

More recently, updated analysis with new DIS data from MARATHON experiment for proton and neutron structure functions confirmed this observation.

D. Abrams, et al. (2022)
S. I. Alekhin, S. A. Kulagin, R. Petti (2022)

Constraining sea quarks $\bar{u}$ and $\bar{d}$ PDFs has the additional complication that they are tangled to the **strangeness** content of the proton.

Strangeness has been constrained using neutrino-nucleon DIS data from NuTeV, and recently new precise data from NOMAD has become available.

S. Alekhin, J. Blümlein, S. Moch (2018)

A direct handle on anti-quark PDFs is provided by the data of the E866 and the recent SeaQuest (E906) experiments; the latter in particular points to a more flat $\bar{d}/\bar{u}$ distribution at large-*x* (*x* up to ~ 0.4)

SeaQuest (2021)
S.Alekhin, J. Blümlein, S. Moch (2018)

The LHC has as well vast potential for PDF constraining:

CMS collaboration (2022)
ATLAS collaboration (2014)

W + charm directly sensitive to proton strangeness content.
NNLO calculations now available,
with a consistent approach to include these data in PDF fits under evaluation.

M. Czakon, et al. (2022)
M. Czakon, et al. (arXiv:2205.11879)

Single top production could also be a good experimental channel to constrain anti-quark PDFs. Available measurements are still too imprecise, but significant improvements can be achieved with future data.

NNPDF collaboration (2022)

The potential of Drell-Yan data

Drell-Yan measurements feature low theoretical and experimental systematics, high statistical precision and good control of correlations.
They can therefore provide strong constraints on PDFs.

We assessed the impact of precision DY measurements on PDF determination from:

- the neutral channel **Forward-Backward Asymmetry (A_{FB})** (aka the angular coefficient **A_4**)
  JF, E. Accomando, et al. (2019)
- the charged channel **Lepton-charge Asymmetry (A_W)**
  JF, F. Giuli, F. Hautmann, S. Moretti (2021)

Direct handle on quark PDFs in wide range of Bjorken-*x*
(rapidity cuts to target high-*x* regions)

Considerable improvements in:
- determination of SM EW parameters JF, F. Giuli, F. Hautmann, S. Moretti (2021)
- sensitivity on BSM new states JF, F. Giuli, F. Hautmann, S. Moretti (2022)
  (narrow, wide and multiple resonant scenarios)

Similar studies performed employing the neutral channel angular coefficient **A_0** :
appears at NLO, sensitive to gluon PDF, implications on Higgs physics
(see backup slides)
JF, S. Amoroso, et al. (2021)

Drell-Yan Asymmetries

Angle ***θ*** defined by the direction between the incoming quark and the lepton in the final state. In pp collisions, the c.o.m. frame is unobservable.

Reconstructed "positive" direction of the incoming quark defined by the boost of the di-lepton system.

$$A_{FB}=\frac{\sigma_F-\sigma_B}{\sigma_F+\sigma_B}$$

At the LHC we can observe the reconstructed A_{FB}^*

$$\sigma_F=\int_0^1\frac{d\sigma}{d\cos\theta}d\cos\theta\ ,\quad \sigma_B=\int_{-1}^0\frac{d\sigma}{d\cos\theta}d\cos\theta$$

PDFs profiling with A_{FB}^* pseudodata:

reduction of uncertainties in sea and valence quarks distributions ($2/3\ u_v + 1/3\ d_v$)

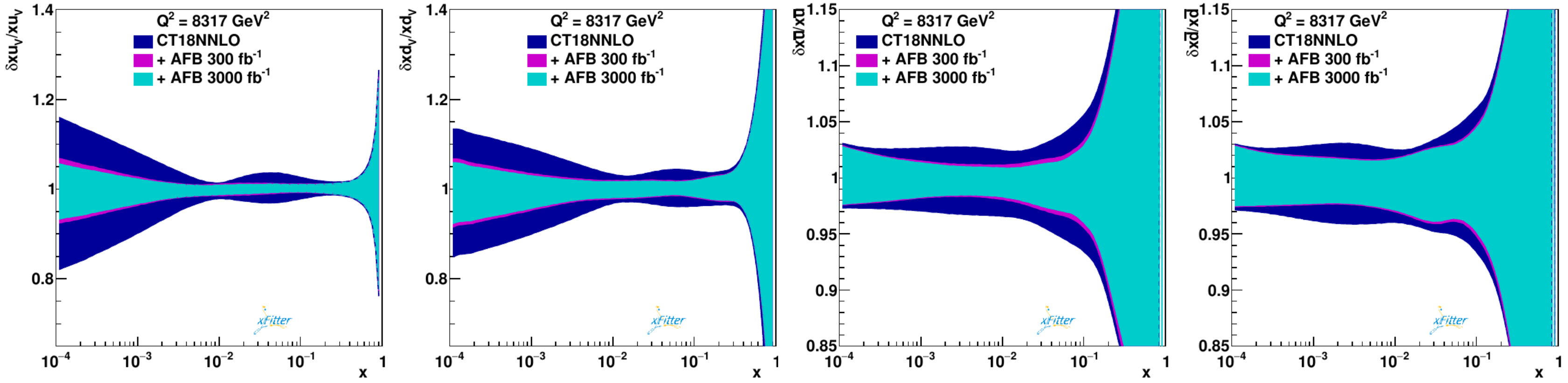

W asymmetry sensitive to independent combination of quark PDFs.

$$A_W=\frac{d\sigma_{W^+}/d\eta_l-d\sigma_{W^-}/d\eta_l}{d\sigma_{W^+}/d\eta_l+d\sigma_{W^-}/d\eta_l}$$

PDFs profiling with A_W pseudodata:

reduction of uncertainties in sea and valence quarks distributions ($d_v - u_v$)

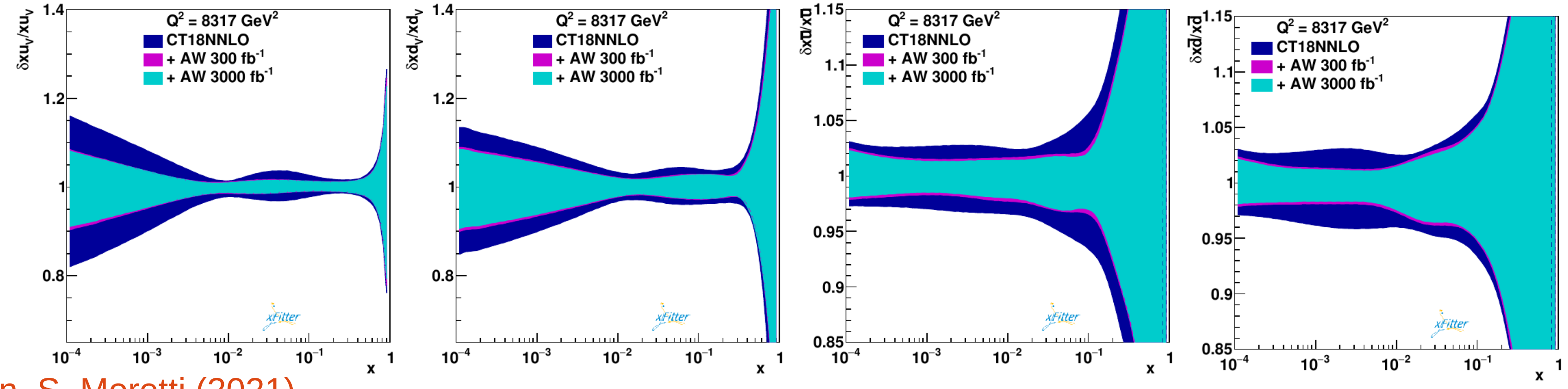

JF, F. Giuli, F. Hautmann, S. Moretti (2021)

BSM high mass searches

Significant reduction of uncertainties in the high invariant/transverse mass spectrum for BSM searches. JF, F. Giuli, F. Hautmann, S. Moretti (2021)

Dilepton high invariant mass:

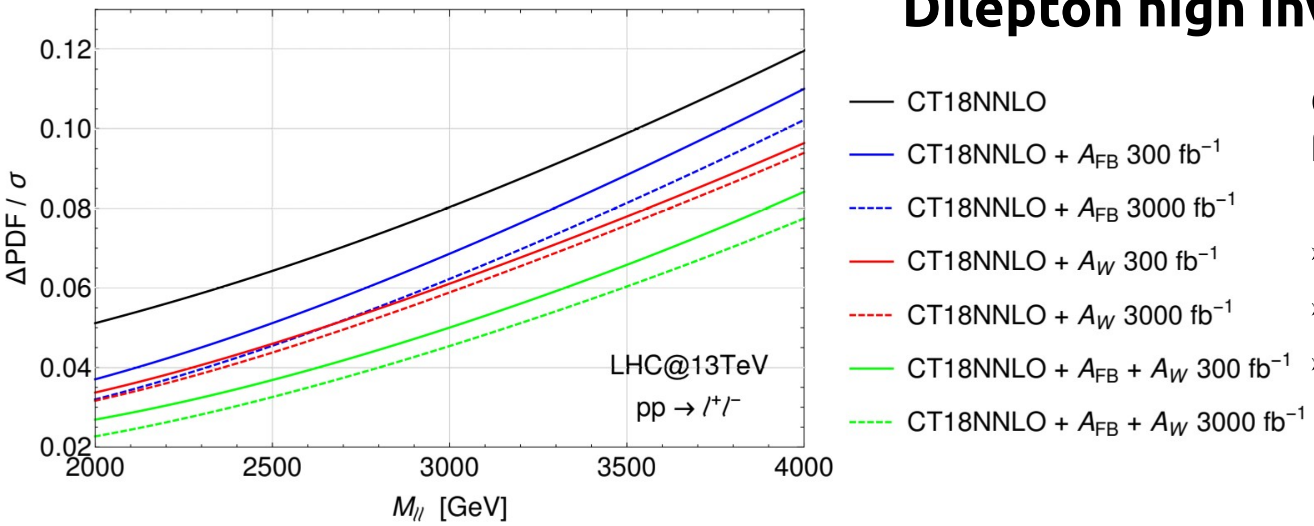

Original PDF uncertainty (i.e.) at 4 TeV from 12% is reduced to:

- 11% (10.2%) by $\mathbf{A_{FB}}$ 300 (3000) fb^{-1} data
- 9.6% (9.4%) by $\mathbf{A_{W}}$ 300 (3000) fb^{-1} data
- 8.4% (7.8%) by combination of $\mathbf{A_{FB}}$ and $\mathbf{A_{W}}$ 300 (3000) fb^{-1} data

Lepton + MET high transverse mass:

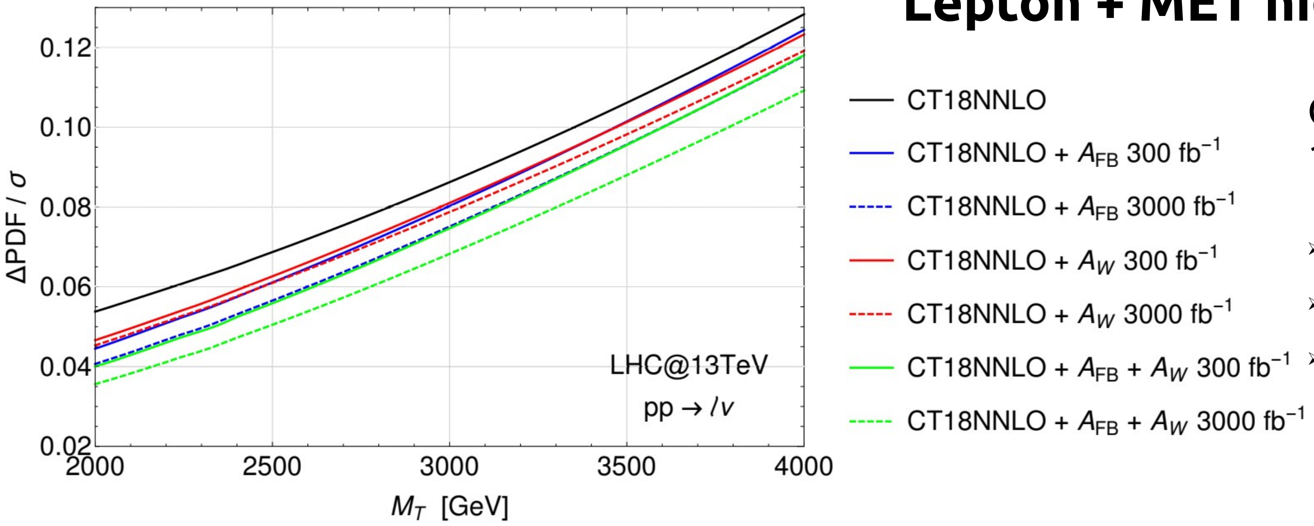

Original PDF uncertainty (i.e.) at 4 TeV from 12.9% is reduced to:

- 12.5% (11.8%) by $\mathbf{A_{FB}}$ 300 (3000) fb^{-1} data
- 12.3% (11.9%) by $\mathbf{A_{W}}$ 300 (3000) fb^{-1} data
- 11.8% (10.9%) by combination of $\mathbf{A_{FB}}$ and $\mathbf{A_{W}}$ 300 (3000) fb^{-1} data

High-x PDF variation

We now concentrate on the high-x quark and anti-quark PDF parametrisation.
To evaluate the uncertainty from the high-x parametrisation we vary the exponents of the (1-x) term in the $\mathbf{u_v}$, $\mathbf{d_v}$, $\bar{\mathbf{u}}$, $\bar{\mathbf{d}}$ distributions at the starting scale $\mu_0^2 = 1.9$ GeV^2

We construct a PDF set as follows:

- Central PDF (member #0) obtained from the results of the ABMP16 fit.

S. Alekhin, J. Blümlein, S. Moch, R. Plačakytė (2017)

- Other members obtained varying the exponents of $\mathbf{u_v}$, $\mathbf{d_v}$, $\bar{\mathbf{u}}$, $\bar{\mathbf{d}}$ distributions **separately** by ± 0.3, 0.5, 1.0
  - 6 variations x 4 exponents = 24 PDF members

- Using these 1+24 PDF members we obtain predictions for the observables (**dσ** and **AFB***) as follows:
  - Central value from member #0
  - 22 predictions from the 24 members: discard the 2 members corresponding to $d_v \rightarrow d_v - 1$ & $u_v \rightarrow u_v - 1$ (d_v/u_v ratio converges to 0 too slowly for $x \rightarrow 1$ to match the observed data)
  - Combining the members with exponents of $\mathbf{u_v}$, $\mathbf{d_v}$, $\bar{\mathbf{u}}$, $\bar{\mathbf{d}}$ distributions **all simultaneously** varied by ± 0.3, 0.5, 1.0:
    - 6 additional predictions (#23 - #28).
    - The cases with variation ±1.0 we name "Variation #1".
  - Combining the members with exponents of $\mathbf{u_v}$ **and** $\mathbf{d_v}$ varied by ±1.0, **while** exponents of $\bar{\mathbf{u}}$, $\bar{\mathbf{d}}$ varied by ∓1.0:
    - 2 additional predictions (#29 - #30).
    - We name these "Variation #2".

We evaluate the uncertainty from high-x parametrisation as the envelope of these 30 predictions.

We are going to consider the impact of this additional source of systematic uncertainty on ***Z'*** **searches in the dilepton channel**.

The differential cross section

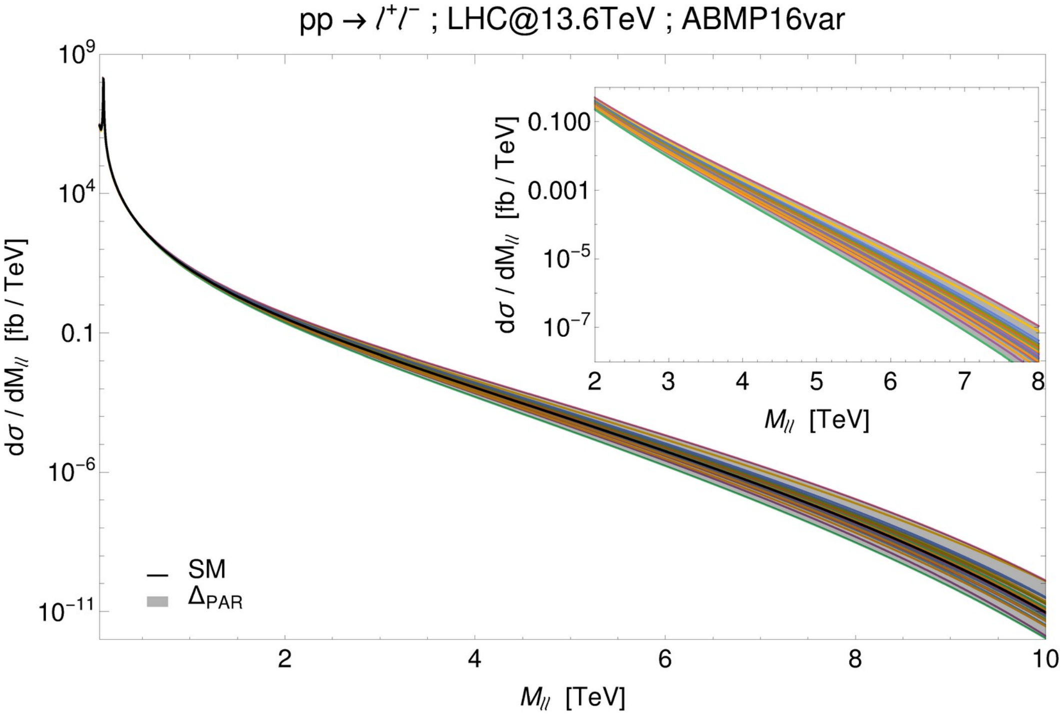

The envelope of the predictions represents an estimation of the uncertainty given by the determination of large-*x* quark PDFs.

For the differential cross section, the largest deviation is obtained with “Variation #1”

The new parametrisation uncertainty results roughly one order of magnitude larger than the traditional PDF uncertainty.

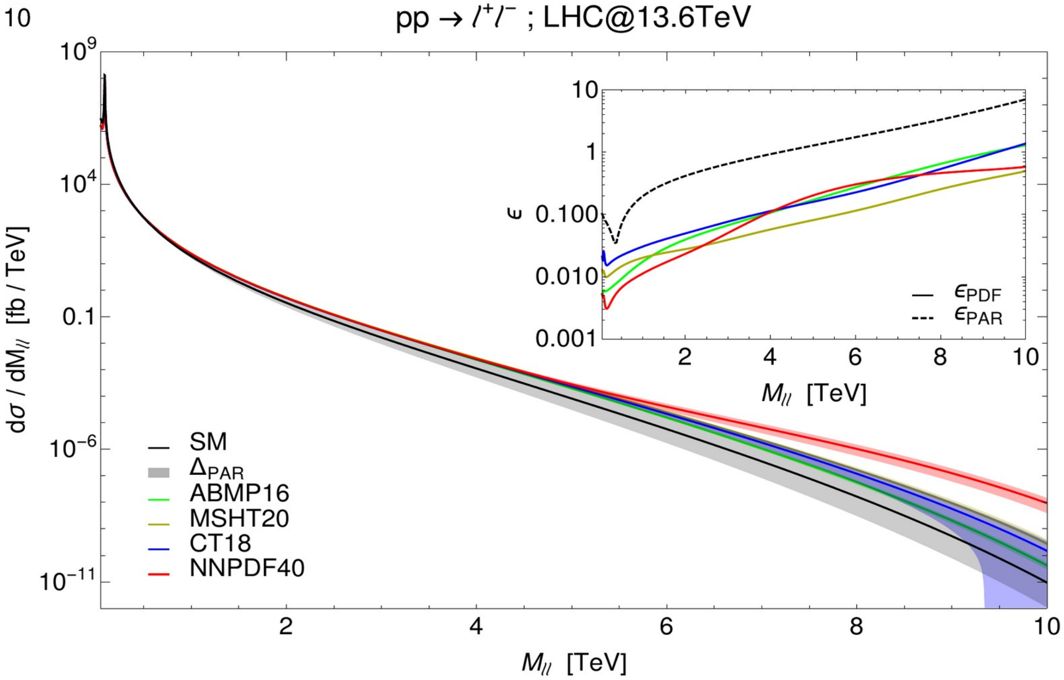

The A_{FB}

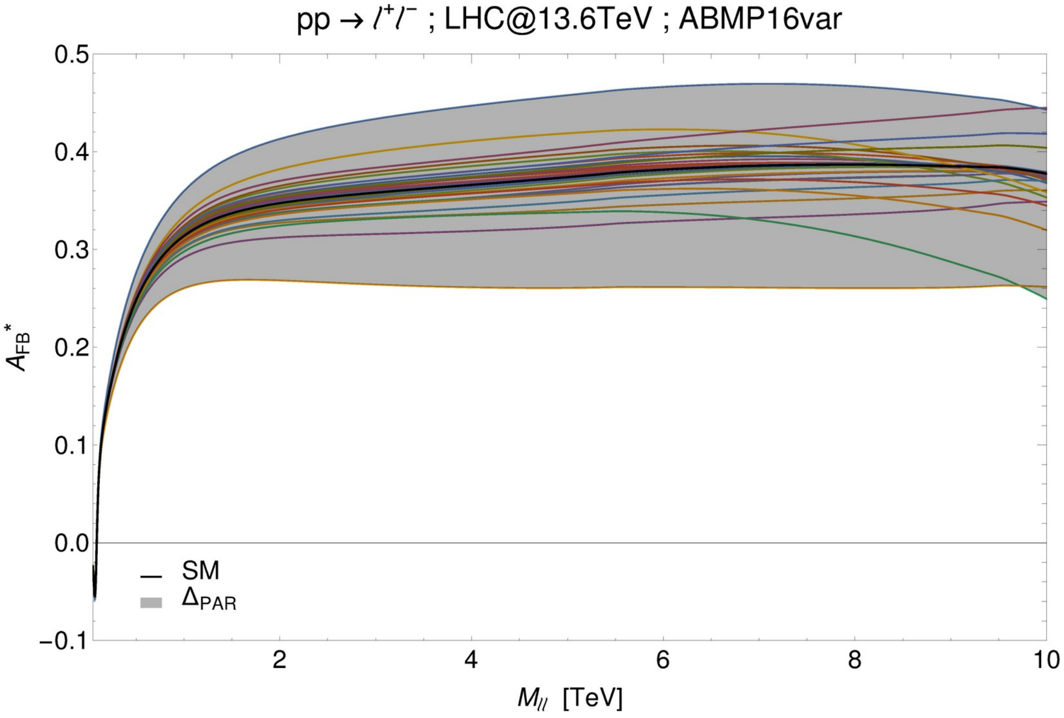

The Forward-Backward Asymmetry results particularly sensitive to the variation of high-*x* quark PDF behaviour.

For this observable, the largest deviation is obtained with "Variation #2"

The parametrisation uncertainty results larger than the traditional PDF uncertainty. It encompasses (for the most part) the predictions obtained with different modern PDF sets.

This behaviour of NNPDF4.0 discussed in

R. D. Ball, et al. (2022)

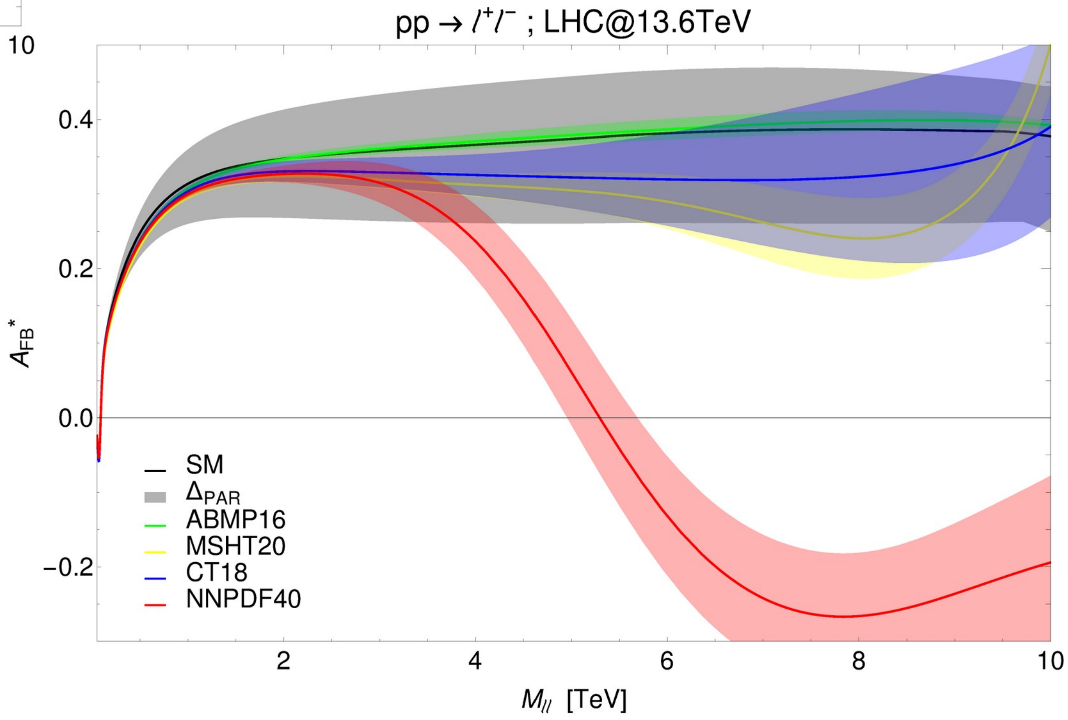

Z’ searches

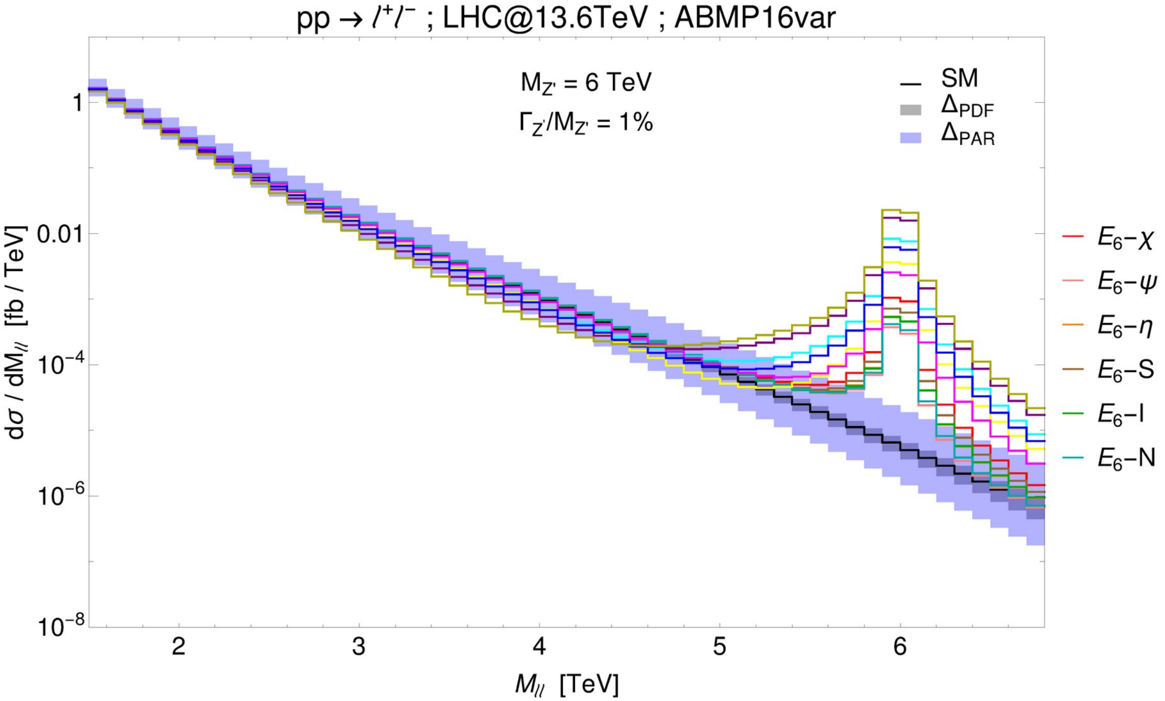

GUT-inspired benchmark models described in E. Accomando, et al. (2011)

The parametrisation error band represents an additional source of systematic error to be accounted for in BSM searches.

Narrow resonances appearing as Breit-Wigner peaks standing over the smooth background maintain well visible signal shapes despite the additional error band.

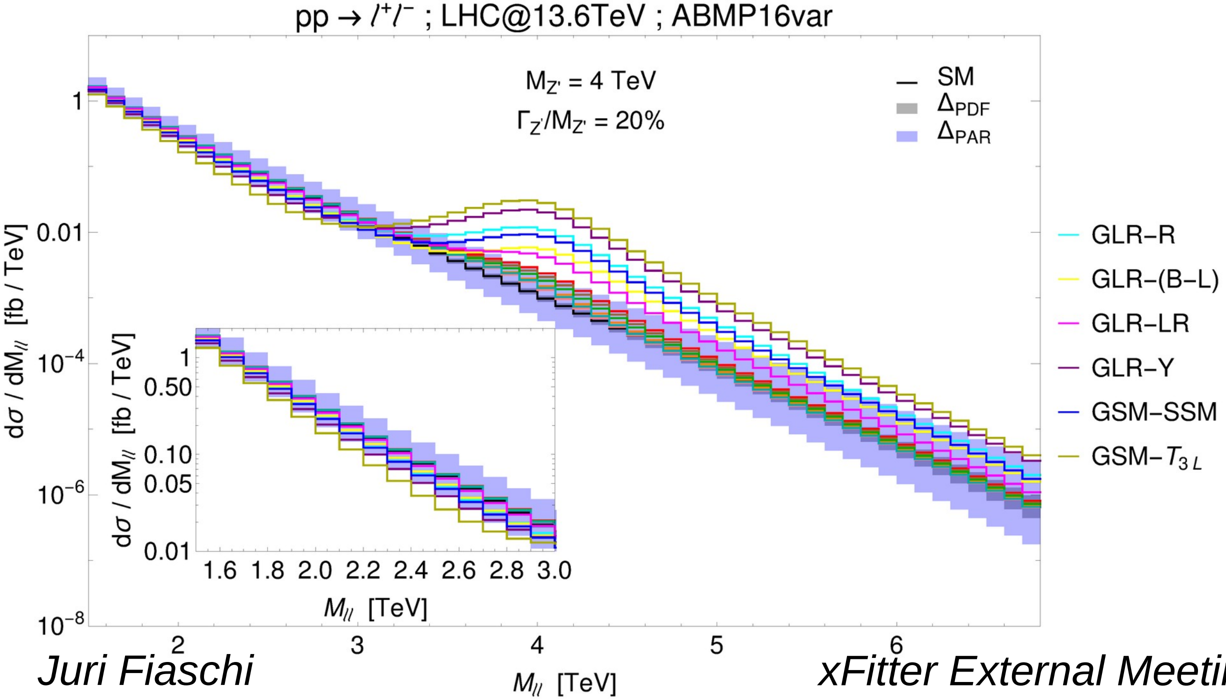

The sensitivity on wide ***Z’*** signals suffers instead a strong reduction.

An interesting feature appearing more visibly in the case of wide resonances concerns the negative interference contribution occurring in the low mass tail of the distribution. The resulting depletion of events can lead to an early indication of the presence of BSM physics.

Z' searches

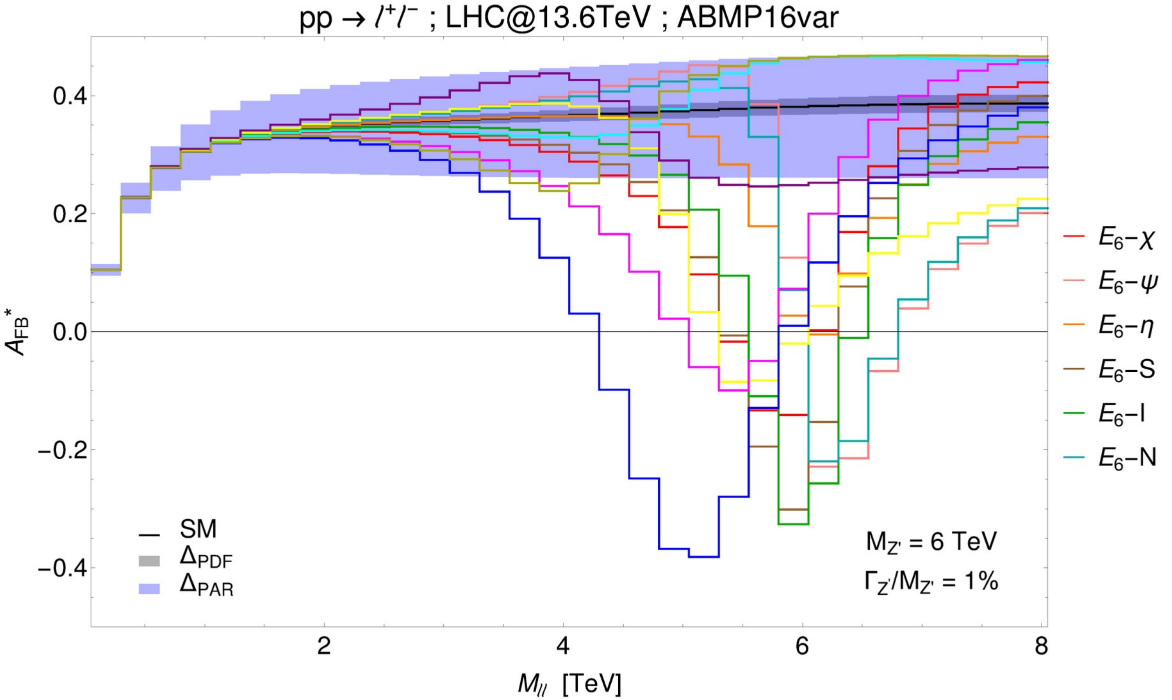

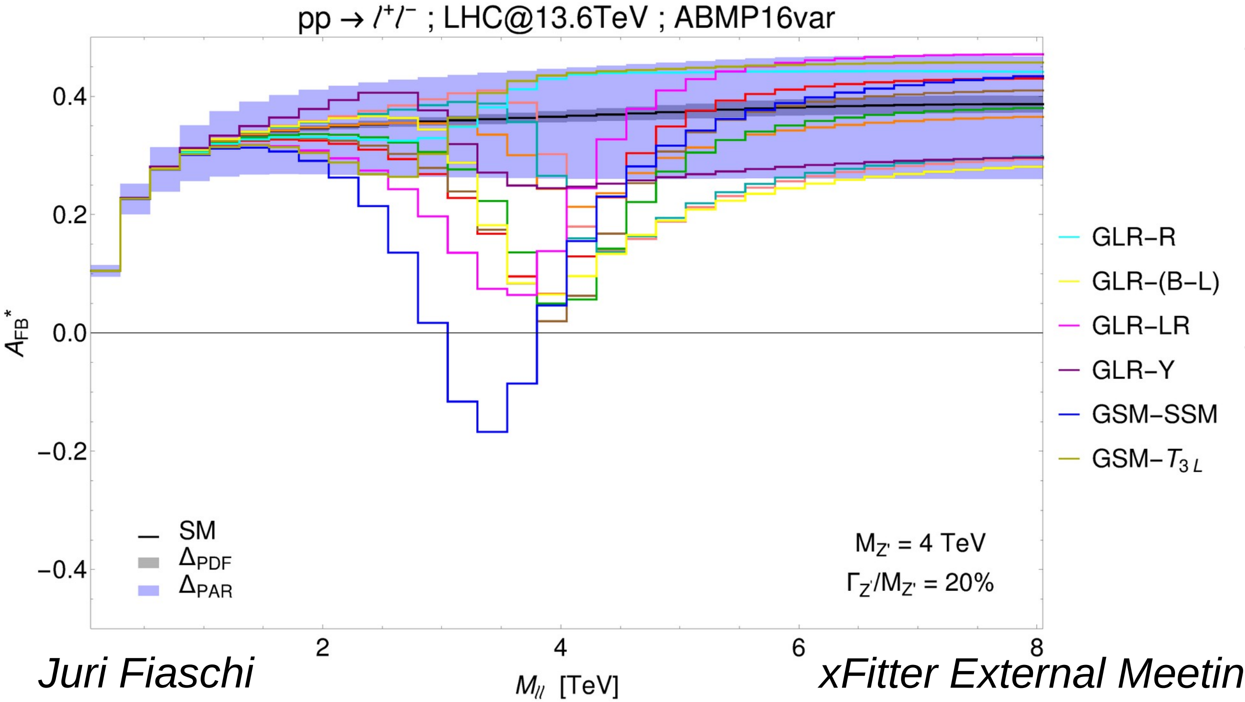

GUT-inspired benchmark models described in E. Accomando, et al. (2011)

The A_{FB} ***Z'*** signal shape remains well visible above the SM background predictions in both scenarios of narrow and wide resonances.

The feature of the A_{FB} of being to some extent unaffected by variations of the resonance width makes this observable a suitable discriminant in BSM searches.

It is however important to remember that this observable, despite its stability against systematic errors, is to large extent overwhelmed by statistical uncertainty.

Case study: wide E_6-I *Z'*

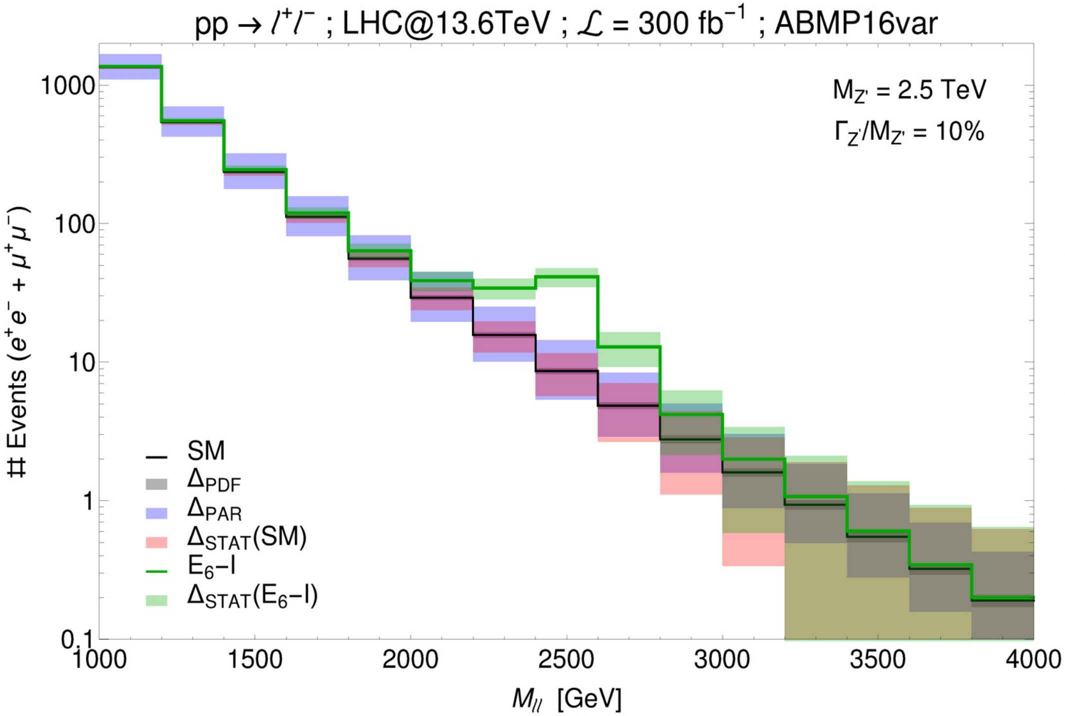

Statistical analysis on a wide ***Z'*** benchmark model:

E_6-I *Z'* with mass of 2.5 TeV and width Γ/M = 10%.

- NNLO corrections included through K-factor (DYTurbo)
- Di-electron and di-muon experimental efficiencies.
- Combined statistic from the two channels.

Benchmark is below current LHC sensitivity, but observable with end of Run-III integrated luminosity in both observables.

- Statistical uncertainty only, significances: **4.4σ** (bump), **4.3σ** (A_{FB}).
- With systematics, significances: **2.9σ** (bump), **2.3σ** (A_{FB}).
- → A combination of the two observables may lead to an early discovery.

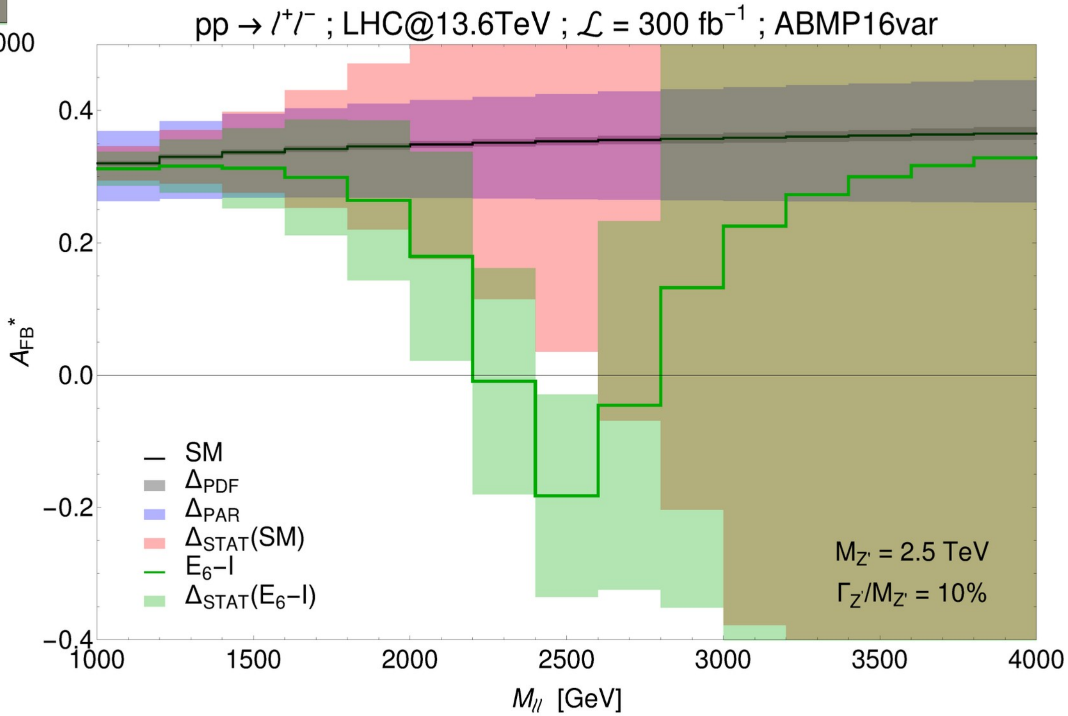

Conclusions

- LHC Run-III provides an unprecedented opportunity to explore high energy scales, where BSM physics may hide.

- Disagreements in the treatment of high-*x* behaviour of quark PDFs shall be addressed. Need to further constrain the light flavour valence and sea content (including strangeness) of the proton.

- Precision measurements at LHC Run-III will allow direct access to high-*x* PDFs. Drell-Yan data in particular gives a direct handle to constrain PDFs in this region (special mention to asymmetries for their partial cancellations of systematics)

- Traditional methods to compute PDF errors do not capture the full extent of high-*x* PDF indetermination. A conservative approach to establish the impact of high-*x* (anti)quark PDFs is adopted.

- BSM searches can be significantly affected by the new systematic error.
  In particular, experimental analyses targeting broad ***Z'*** signals may suffer a strong reduction of sensitivity.

- Employing additional observables such as the $\mathbf{A_{FB}}$, can improve the overall sensitivity of BSM experimental searches.

Thank you!

Backup slides

Neutral Drell-Yan

Expansion of the full differential cross section in therms of the angular coefficients **A**$_i$:

$$\frac{\mathrm{d}\sigma}{\mathrm{d}p_{\mathrm{T}}^{Z}\,\mathrm{d}y^{Z}\,\mathrm{d}m^{Z}\,\mathrm{d}\cos\theta\,\mathrm{d}\phi} = \frac{3}{16\pi}\frac{\mathrm{d}\sigma^{U+L}}{\mathrm{d}p_{\mathrm{T}}^{Z}\,\mathrm{d}y^{Z}\,\mathrm{d}m^{Z}}$$

Unpolarised cross-section

$$\Big\{(1+\cos^2\theta)+\frac{1}{2}\underline{A_0}(1-3\cos^2\theta)+A_1\,\sin 2\theta\,\cos\phi$$

Helicity cross-sections

$$+\frac{1}{2}A_2\,\sin^2\theta\,\cos 2\phi+A_3\,\sin\theta\,\cos\phi+\underline{A_4}\,\cos\theta$$

$$+A_5\,\sin^2\theta\,\sin 2\phi+A_6\,\sin 2\theta\,\sin\phi+A_7\,\sin\theta\,\sin\phi\Big\}.$$

JF, F. Giuli, F. Hautmann, S. Moretti (2021)

E. Accomando, et al. (2019)

Angles measured in the Collins-Soper frame

Drell-Yan angular coefficients

$< 1 + \cos^2\theta >$	Normalization of the unpolarised cross-section
$< \frac{1}{2}(1-3\cos^2\theta) >= \frac{3}{20}(A_0 - \frac{2}{3})$	Longitudinal polarisation
$< \sin 2\theta \ \cos\phi >= \frac{1}{5} A_1$	Interference term: longitudinal/transverse
$< \sin^2\theta \ \cos 2\phi >= \frac{1}{10} A_2$	Transverse polarisation
$< \sin\theta \ \cos\phi >= \frac{1}{4} A_3$	Product of V-A couplings, sensitive to the Weinberg angle
$< \cos\theta >= \frac{1}{4} A_4$	8/3*A_{FB}, non-zero at LO
$< \sin^2\theta \ \sin 2\phi >= \frac{1}{5} A_5$	Zero at NLO, first contributions at NNLO
$< \sin 2\theta \ \sin\phi >= \frac{1}{5} A_6$	
$< \sin\theta \ \sin\phi >= \frac{1}{4} A_7$	

$$\left\langle P(\cos\theta,\phi)\right\rangle = \frac{\int P(\cos\theta,\phi)\, d\sigma(\cos\theta,\phi)\, d\cos\theta\, d\phi}{\int d\sigma(\cos\theta,\phi)\, d\cos\theta\, d\phi}$$

ABMP16 fit

Parametrisation:

$$xq_v(x,\mu_0^2) \;=\; \frac{2\delta_{qu}+\delta_{qd}}{N_q^v}x^{a_q}(1-x)^{b_q}x^{P_{qv}(x)}$$

$$xq_s(x,\mu_0^2) \;=\; x\bar{q}_s(x,\mu_0^2) = A_{qs}(1-x)^{b_{qs}}x^{a_{qs}P_{qs}(x)}$$

$$xg(x,\mu_0^2) \;=\; A_g x^{a_g}(1-x)^{b_g}x^{a_g P_g(x)}$$

$$P_p(x) \;=\; (1+\gamma_{-1,p}\ln x)\left(1+\gamma_{1,p}x+\gamma_{2,p}x^2+\gamma_{3,p}x^3\right)$$

ABMP16 fit:

S. Alekhin, J. Blümlein, S. Moch, R. Plačakytė (2017)

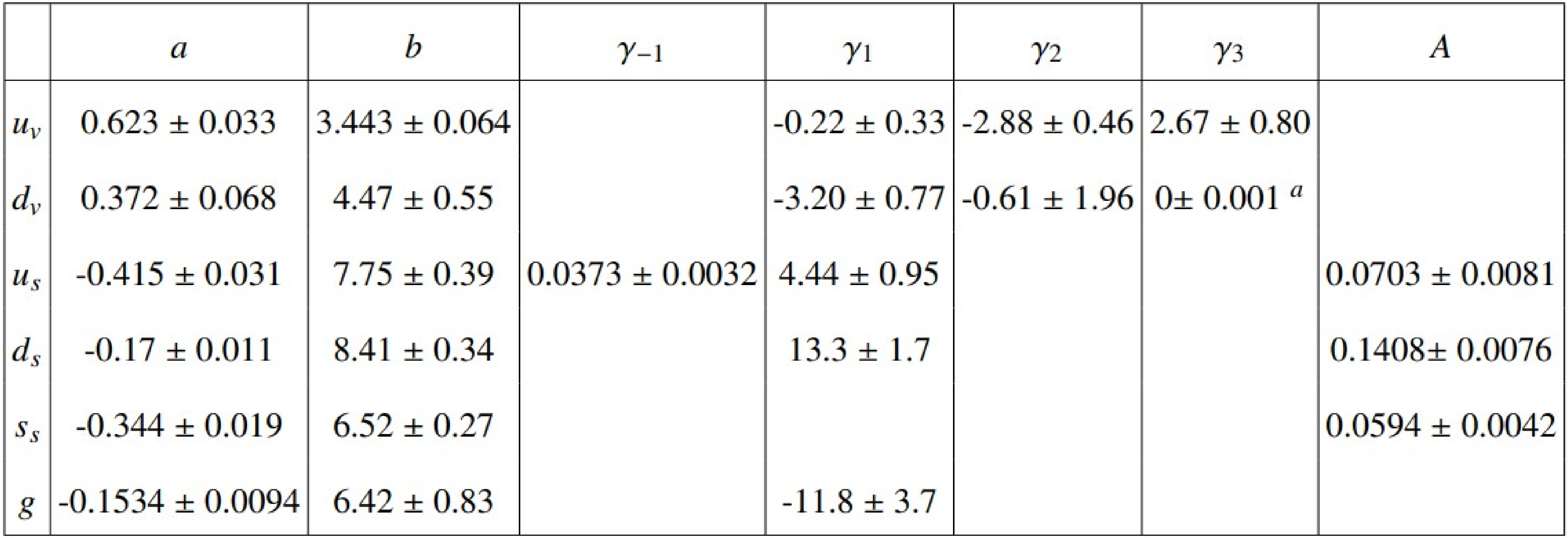

	a	b	γ_{-1}	γ_1	γ_2	γ_3	A
u_v	0.623 ± 0.033	3.443 ± 0.064		-0.22 ± 0.33	-2.88 ± 0.46	2.67 ± 0.80	
d_v	0.372 ± 0.068	4.47 ± 0.55		-3.20 ± 0.77	-0.61 ± 1.96	0± 0.001 [a]	
u_s	-0.415 ± 0.031	7.75 ± 0.39	0.0373 ± 0.0032	4.44 ± 0.95			0.0703 ± 0.0081
d_s	-0.17 ± 0.011	8.41 ± 0.34		13.3 ± 1.7			0.1408± 0.0076
s_s	-0.344 ± 0.019	6.52 ± 0.27					0.0594 ± 0.0042
g	-0.1534 ± 0.0094	6.42 ± 0.83		-11.8 ± 3.7			

Quark & gluon PDFs and evolution

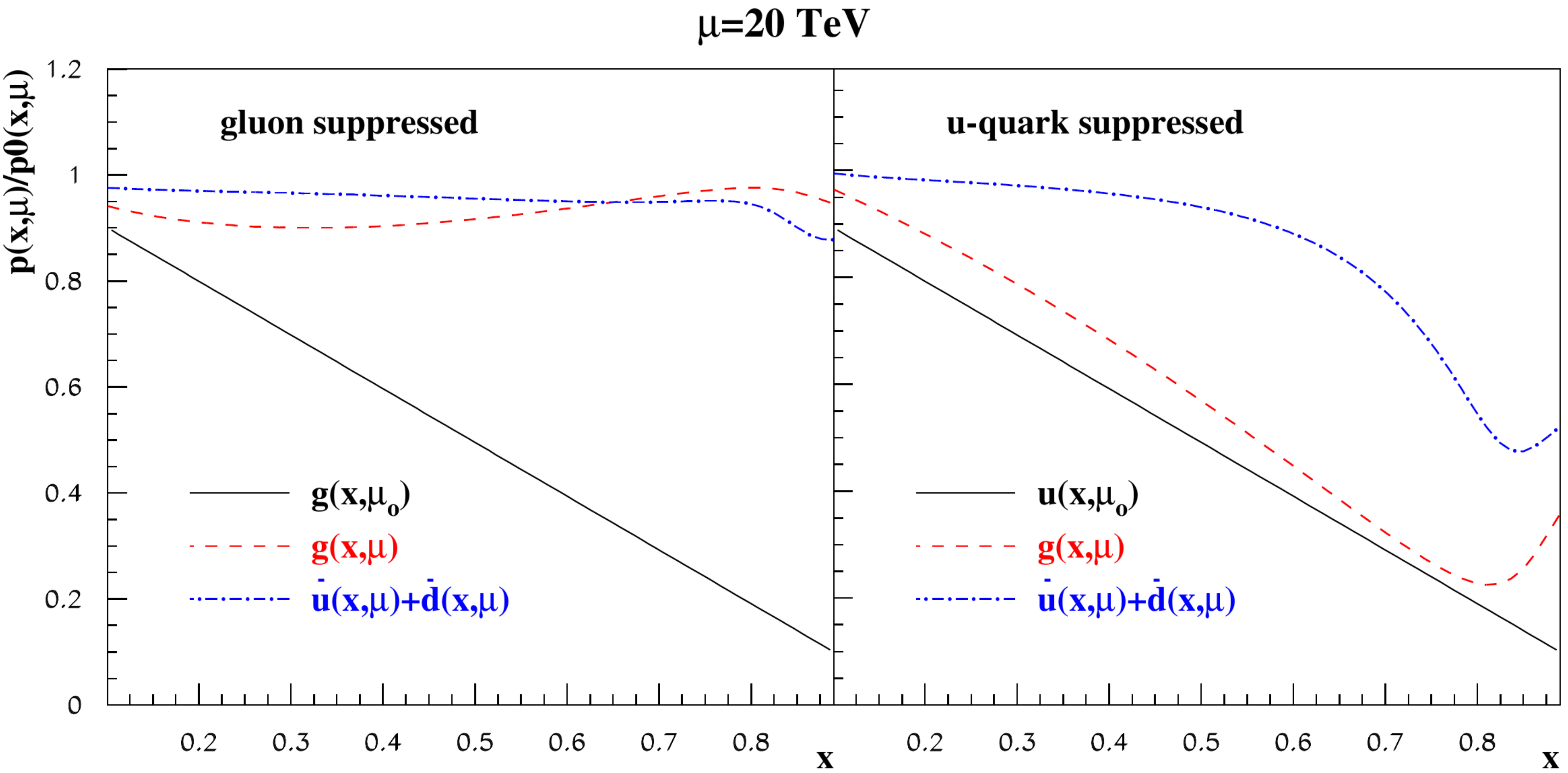

Response of the gluon and sea distributions evolved from the factorization scale μ_0 = 3 GeV to μ = 20 TeV to the suppression of the initial gluon distribution (left panel) and up-quark distribution (right panel) by a factor of (1– x) given as a ratio of PDFs.

S. Alekhin, J. Blümlein, S. Moch, R. Plačakytė (2017)

d_v / u_v

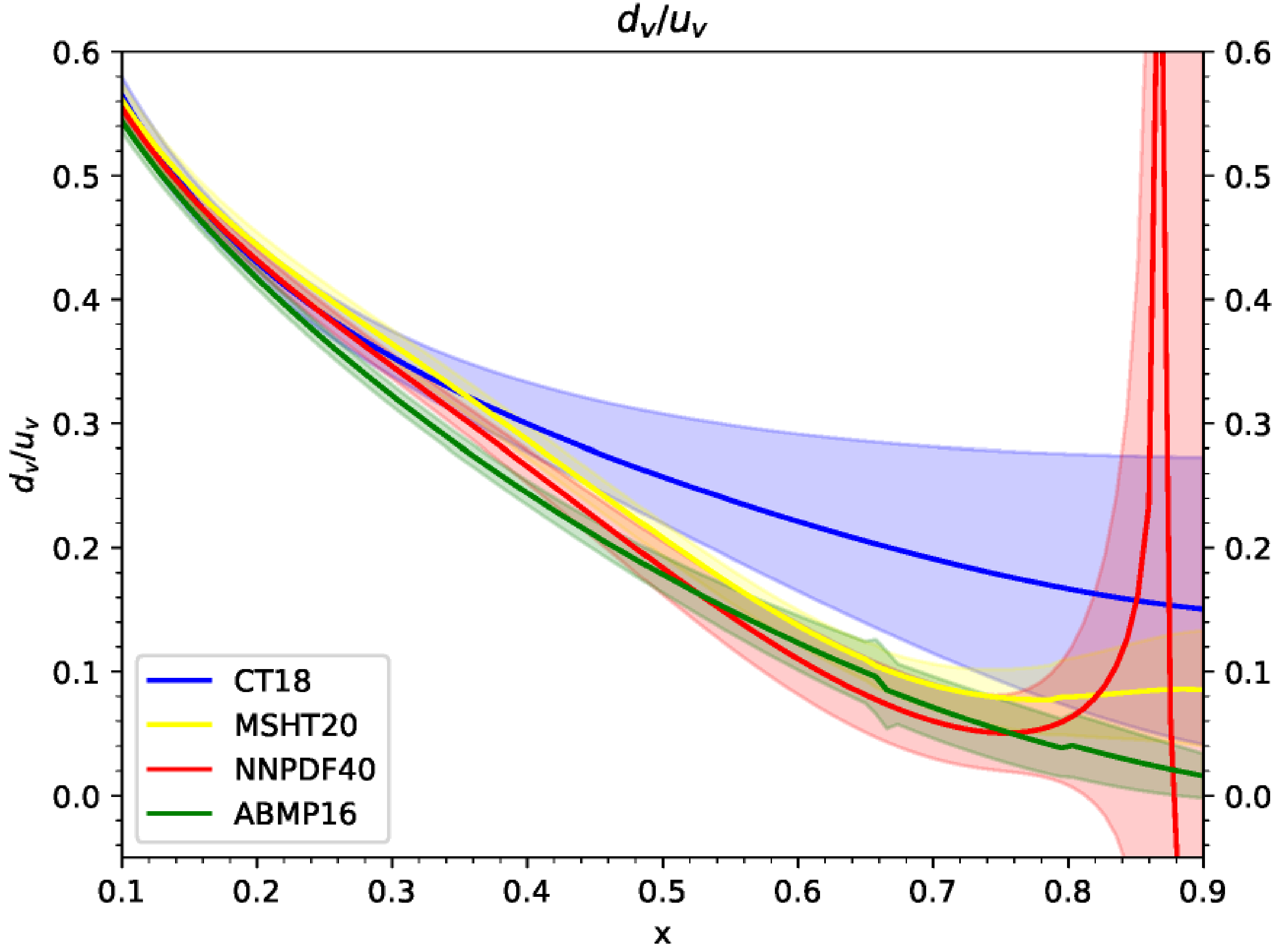
d_v/u_v
d_v/u_v
x
0.6
0.5
0.4
0.3
0.2
0.1
0.0
0.1
0.2
0.3
0.4
0.5
0.6
0.7
0.8
0.9
CT18
MSHT20
NNPDF40
ABMP16

Profiling with A_{FB}

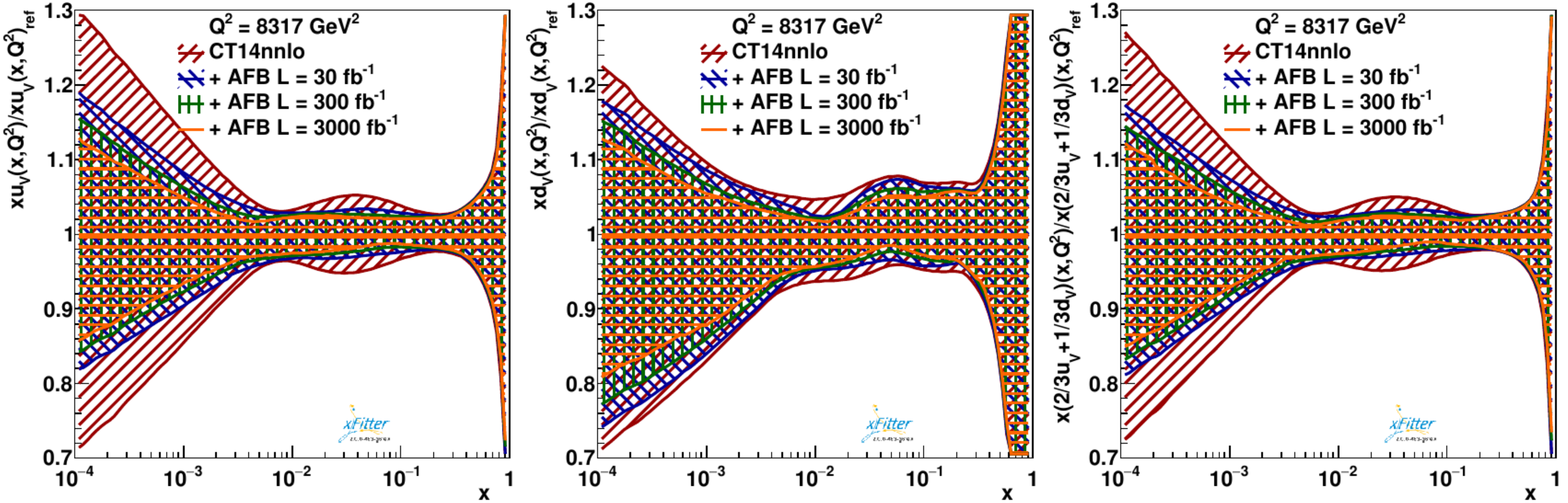

- **A_{FB}** (related to the angular coefficient $A_4 = 8/3\ A_{FB}$) is parity violating and sensitive to the flavor non-singlet PDFs.

- Sensitive to **$\sin^2\theta_W$** however the results of the analysis are rubust against variations in the choice of this parameter.

- The profiling with A_{FB} pseudodata leads to large reductions of uncertanty on *u* and *d* valence quarks PDFs, and particularly on the linear combination **$2/3u_V + 1/3d_V$** .

- Improvement is concentrated in low and intermediate Bjorken *x* regions.

JF, E. Accomando, et al. (2019)

A_{FB} eigenvector rotation

Assess the single PDF sensitivity on A_{FB} data through eigenvector rotation exercise:

J. Pumplin (2009)

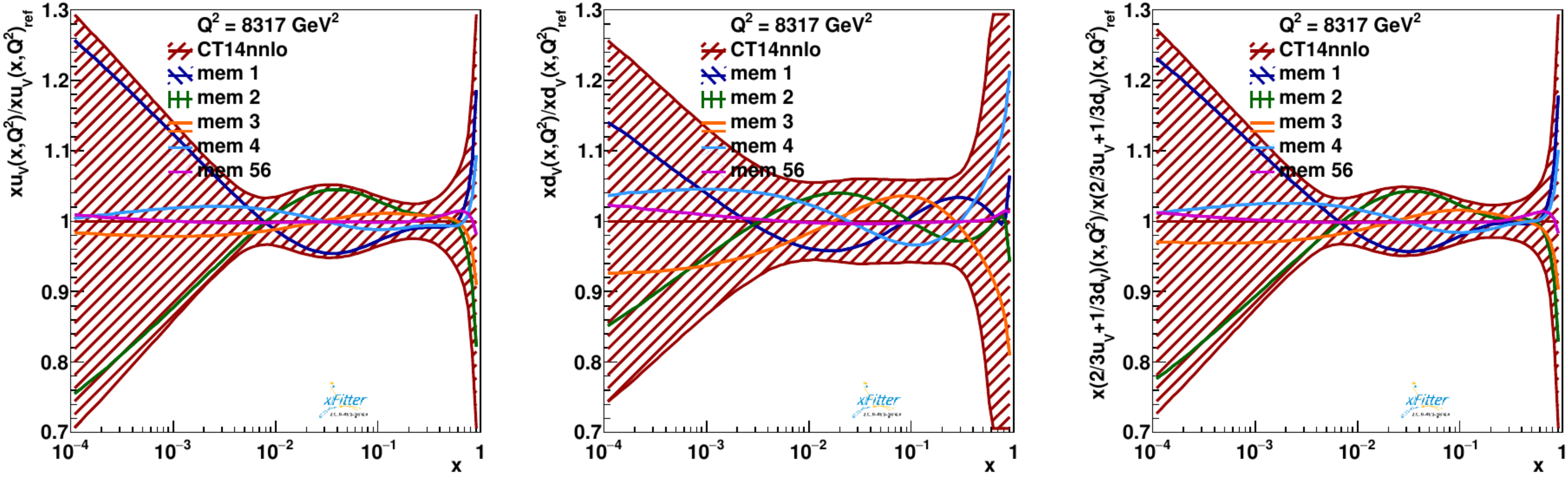

- Eigenvectors rotated and sorted according to their sensitivity to the new data.
- First pair or eigenvectors almost completely saturate the error bands.
- Largest sensitivity on valence quarks, particularly on the combination **$(1/3\ d_V + 2/3\ u_V)$**

JF, E. Accomando, et al. (2019)

Profiling with A_{FB}

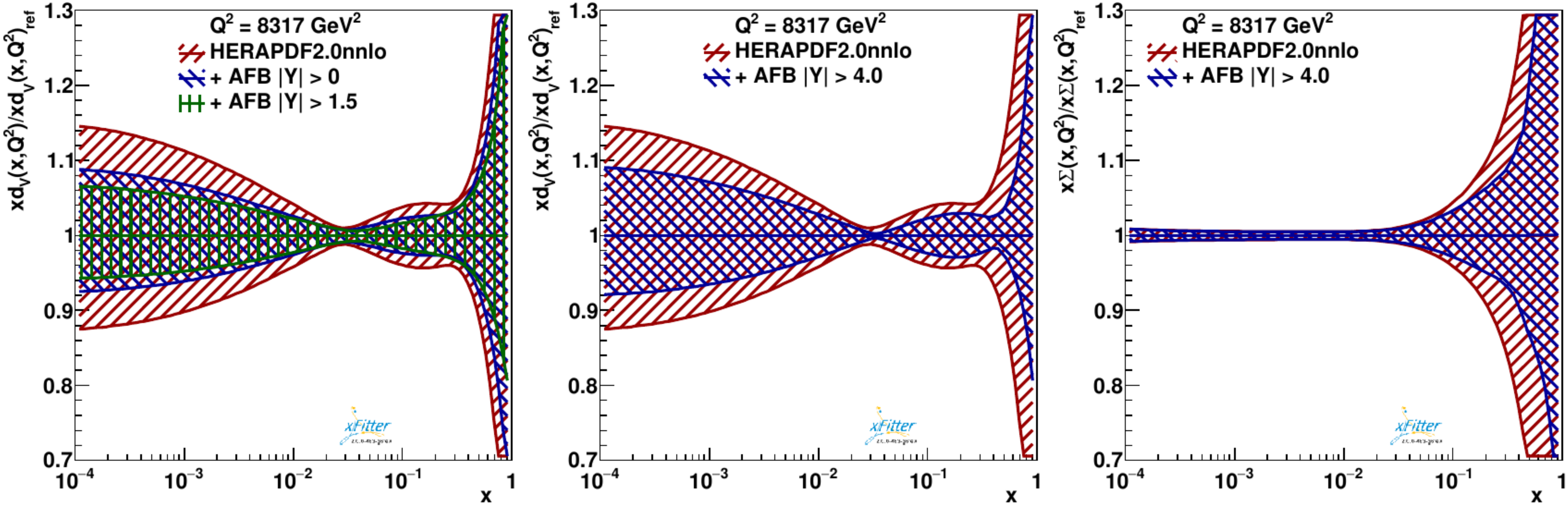

L = 3000 fb^{-1}

- High-x regions can be accessed applying specific rapidity cuts.
- Remarkable improvement in valence and sea quark distributions for $x > 10^{-1}$ when employing A_{FB} pseudodata in the very high rapidity region.
- The reduced statistic due to the strong rapidity cuts requires high integrated luminosity.

JF, E. Accomando, et al. (2019)

A_W vs A_{FB}

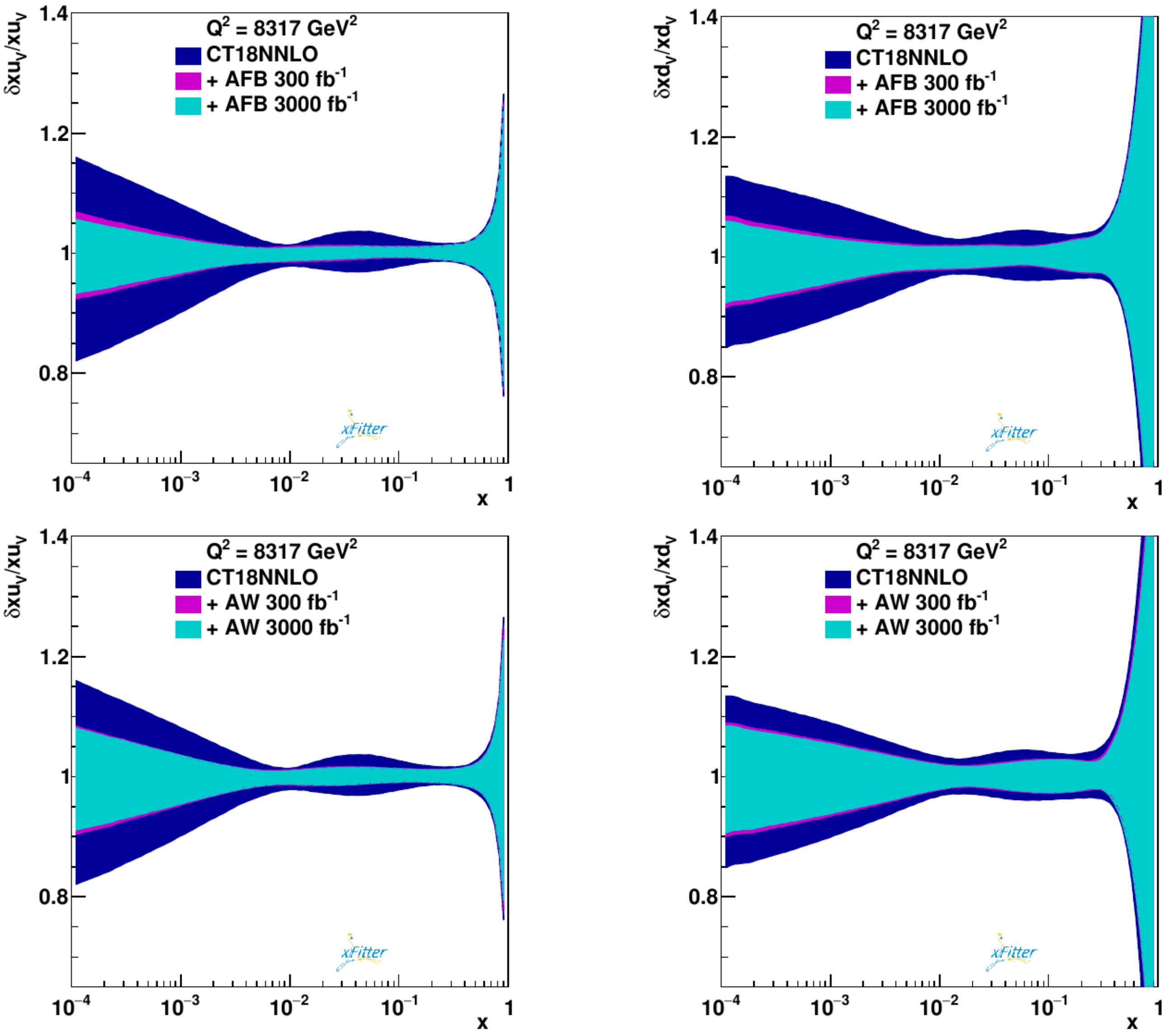

CT18NNLO + A_{FB}

CT18NNLO + A_W

JF, F. Giuli, F. Hautmann, S. Moretti (2021)

Comparable sensitivity on valence quark PDFs, with **A_{FB}** providing slightly stronger constraints.

Saturation of uncertainty reduction from 300 fb^{-1} to 3000 fb^{-1}.

A_W vs A_{FB}

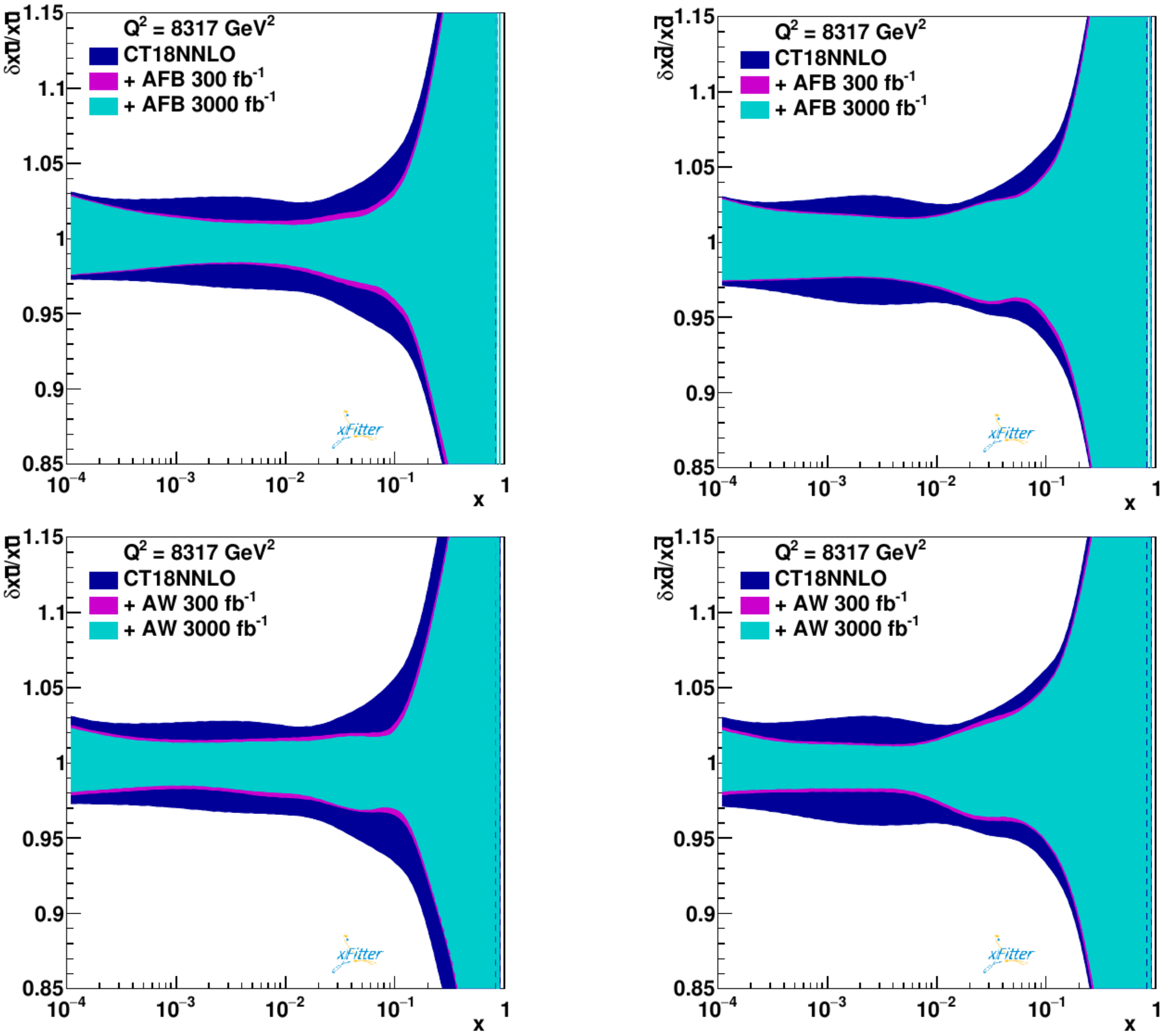

CT18NNLO + A_{FB}

CT18NNLO + A_W

JF, F. Giuli, F. Hautmann, S. Moretti (2021)

A_W provides slightly stronger than **A_{FB}** on anti-quark PDFs, particularly for $\bar{u}$ in the low x region and for $\bar{d}$ in the low and intermediate x range.

Combining A_W and A_{FB}

CT18NNLO + A_{FB} + A_W

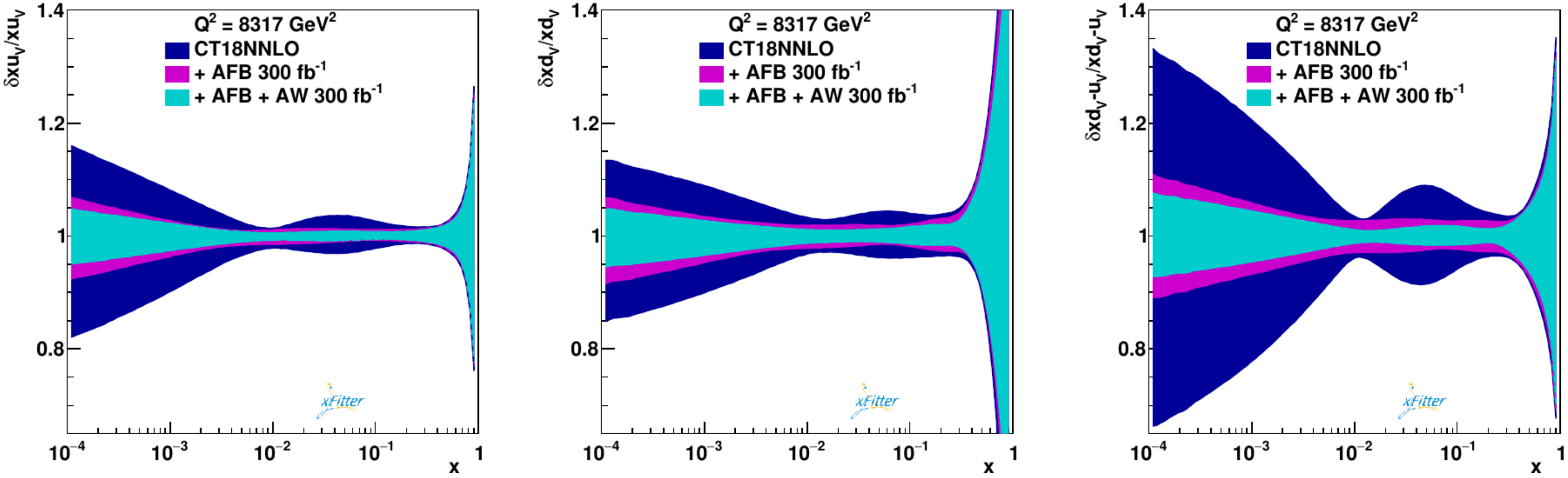

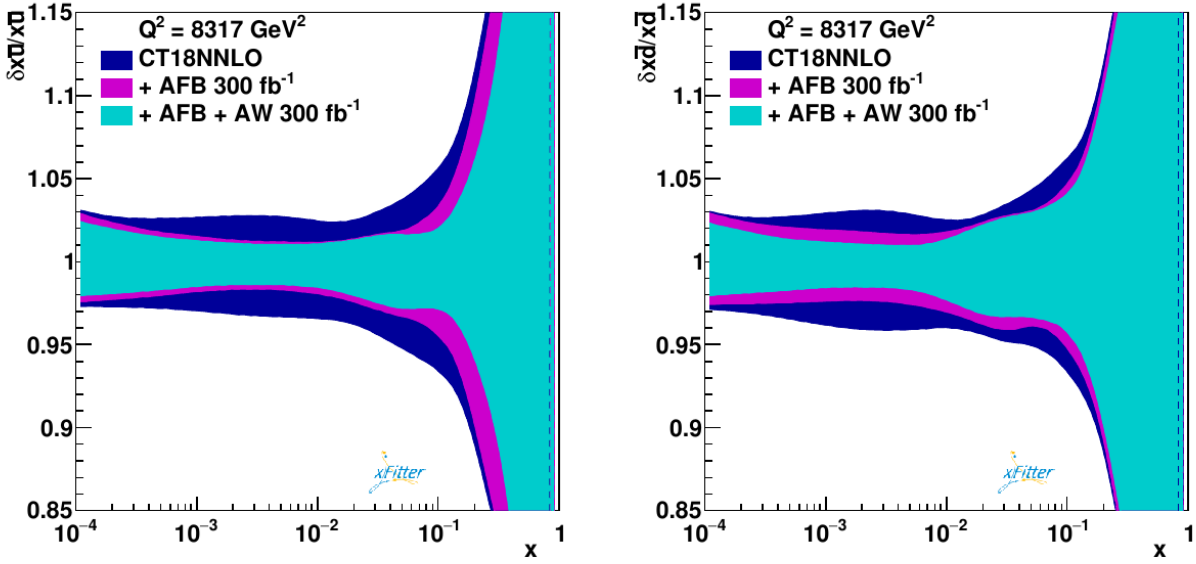

Saturation of uncertainty reduction from 300 fb^{-1} to 3000 fb^{-1}.

- Visible reduction in valence quark PDFs in low and intermediate x region.
- **A_W** most sensitive to the combination **$d_v - u_v$** .
- The combination of **A_W** and **A_{FB}** can further reduce the PDF error bands.
- Large reduction in $\bar{u}$ PDF in the high *x* region and in $\bar{d}$ PDF in the intermediate *x* region.

JF, F. Giuli, F. Hautmann, S. Moretti (2021)

BSM resonances detection

PDF uncertainties are relevant in searches for non-resonant objects.

Benchmark: Enhanced SSM model
(same as SSM with BSM gauge coupling augmented by factor 3)

JF, E. Accomando, et al. (2020)

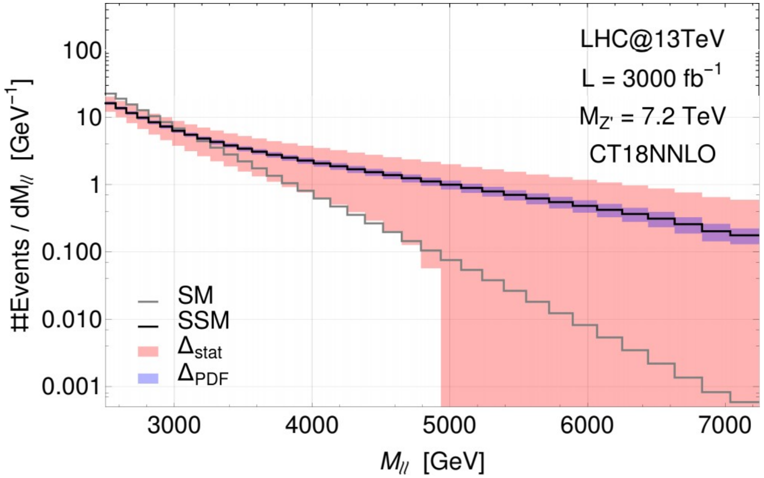

High invariant mass excess is non-significant

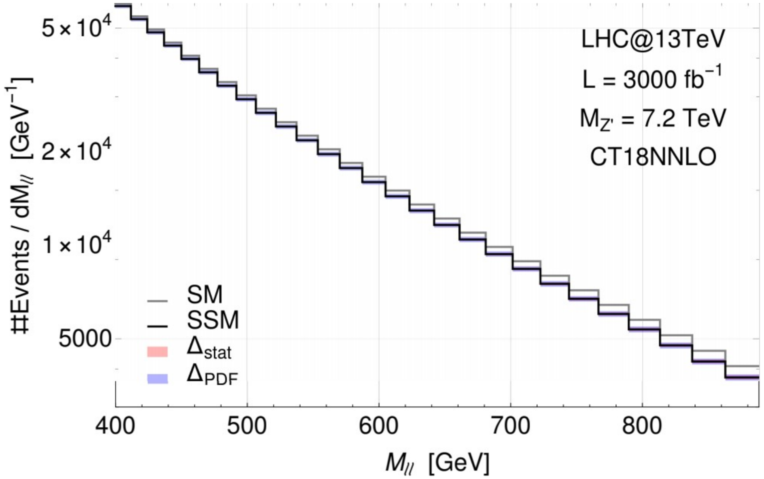

Significant depletion of events due to interference in the low invariant mass tail

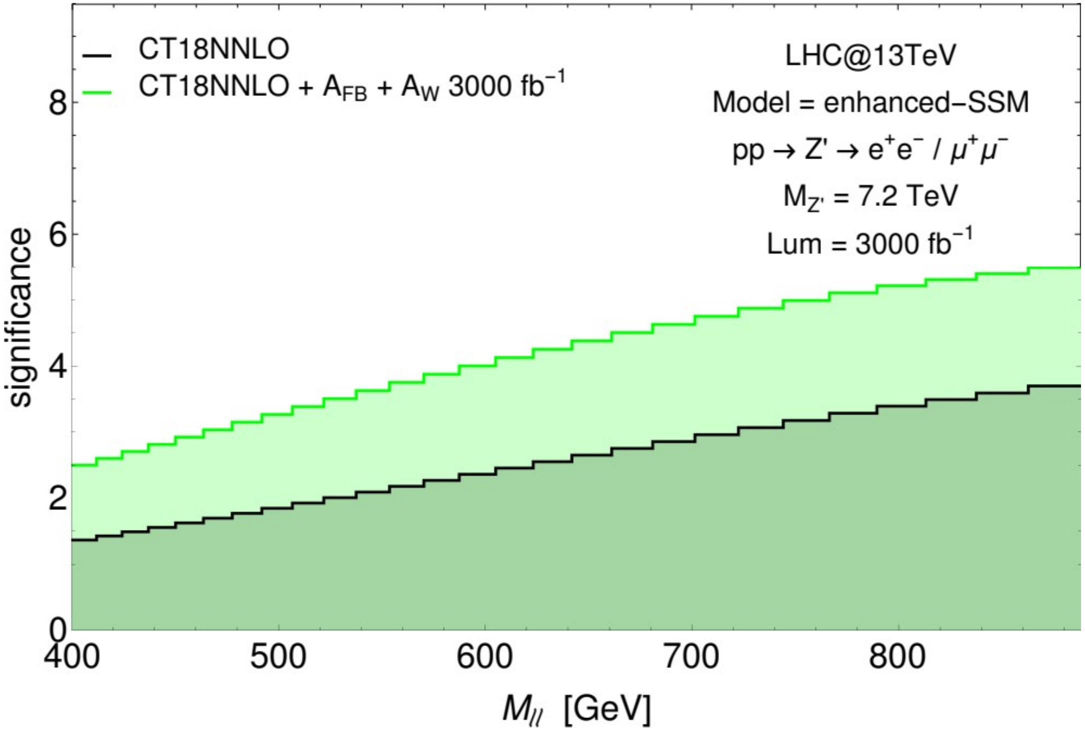

Early evidence of BSM physics significantly improved by reduction of PDF uncertainty

A_W for proton antimatter asymmetry

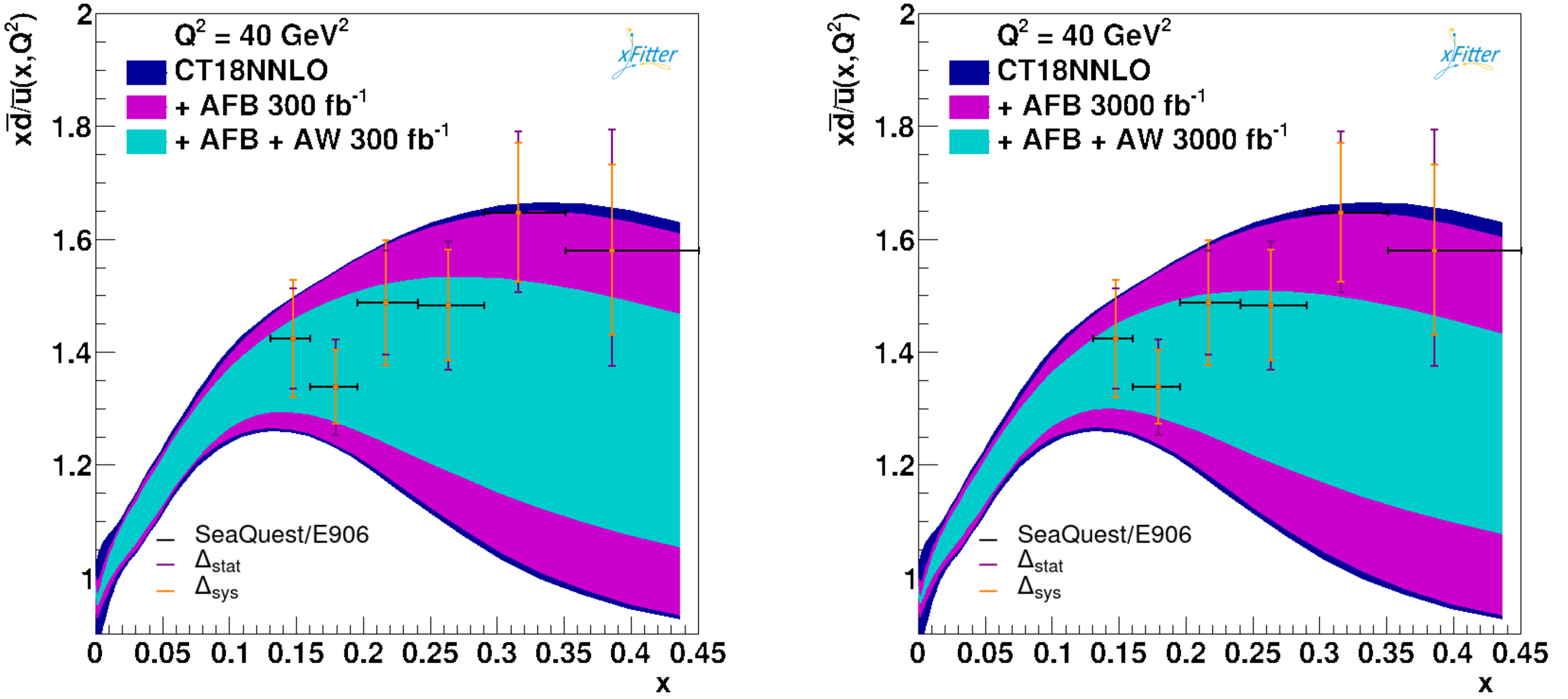

SeaQuest (2021)

A_W data carries relevant information on the anti-quark PDFs in the high x region, and would provide a significant reduction of uncertainty bands in the region of interest.

(REMARK: real data would most certainly modify the central values as well)

JF, F. Giuli, F. Hautmann, S. Moretti (2021)

A_{FB}

$$\sigma_F = \int_0^1 \frac{d\sigma}{d\cos\theta} d\cos\theta \quad , \quad \sigma_B = \int_{-1}^0 \frac{d\sigma}{d\cos\theta} d\cos\theta$$

$$\boxed{A_{FB} = \frac{\sigma_F - \sigma_B}{\sigma_F + \sigma_B}}$$

The angle ***θ*** is defined as the direction between the incoming quark and the lepton in the final state.
In pp collisions, the c.o.m. frame is unobservable.

At the LHC we can observe the reconstructed AFB*

At LO the direction of the incoming quark is defined by the boost of the di-lepton system.

At NLO the angle is defined in the Collins-Soper frame.

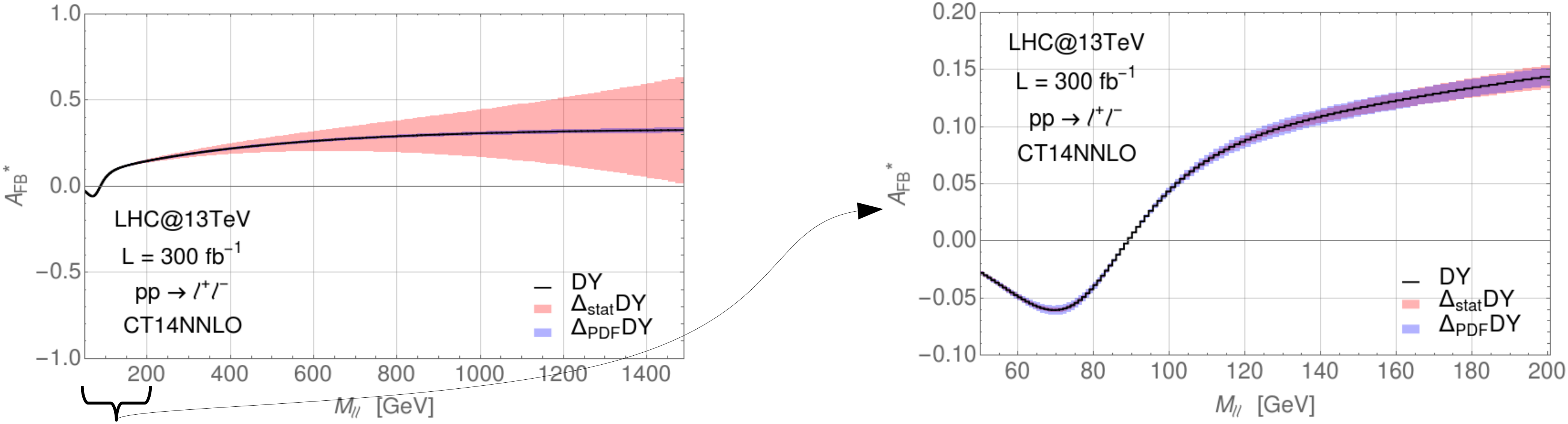

AFB has smaller systematic but larger statistical error compared to cross section measurements.

- High-invariant mass region: dominated by statistical uncertainties.
- Z peak region: high-stats to perform very precise measurements.

Neutral channel asymmetry

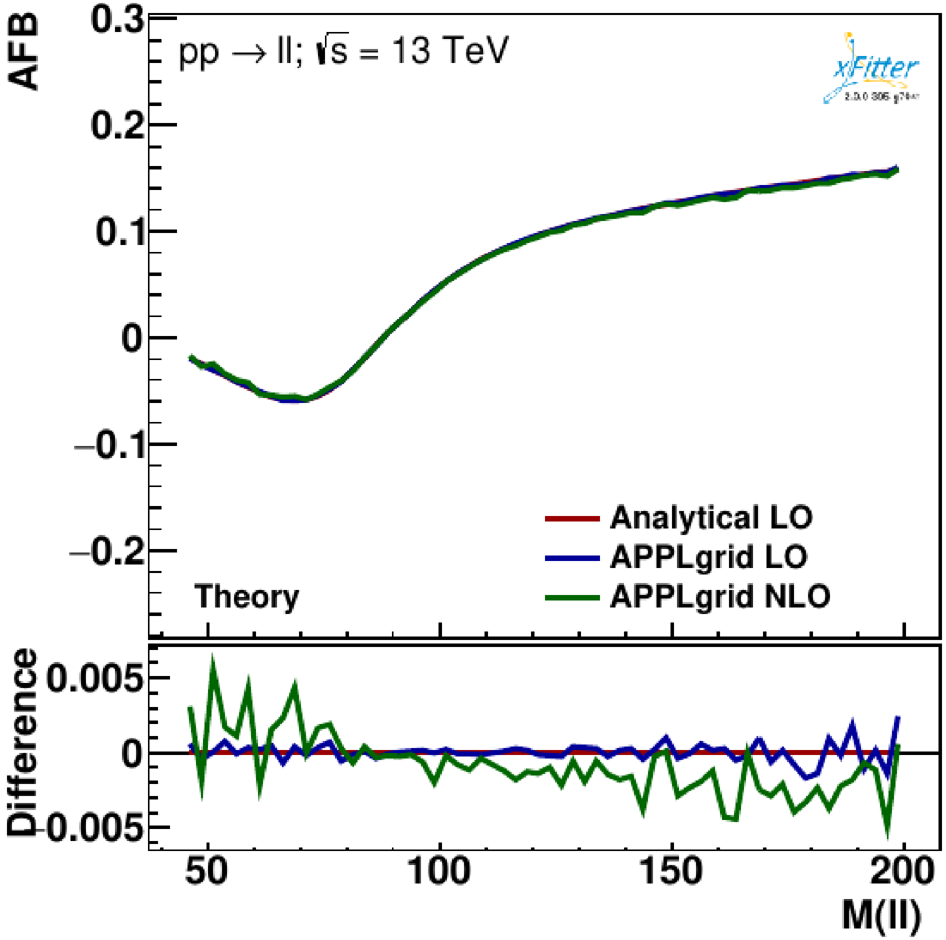

Radiative corrections are small.

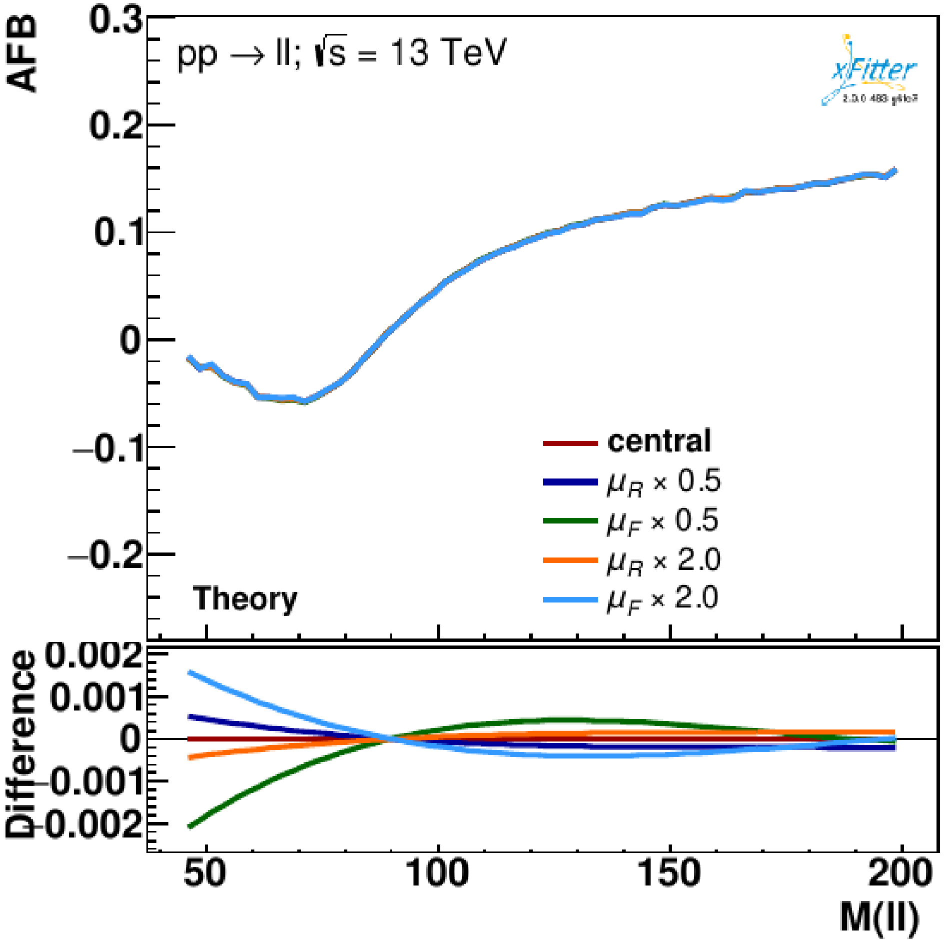

Theory uncertainty from
scale variation under control.

The Lepton-charge asymmetry

$$A_W = \frac{d\sigma_{W^+}/d\eta_\ell - d\sigma_{W^-}/d\eta_\ell}{d\sigma_{W^+}/d\eta_\ell + d\sigma_{W^-}/d\eta_\ell}$$

Calculations at **NLO QCD** accuracy, supplemented with **NNLO QCD** correction through **K-factor**.

Modern PDF sets well describe A_W data

PDF set	χ^2**/d.o.f.**
CT18NNLO	10.26/11
CT18ANNLO	11.29/11
MSHT20nnlo_as118	12.18/11
NNPDF3.1_nnlo_as_0118_hessian	14.88/11
PDF4LHC15_nnlo_100	9.53/11
ABMP16_5_nnlo	18.21/11
HERAPDF20_NNLO_EIG	8.92/11

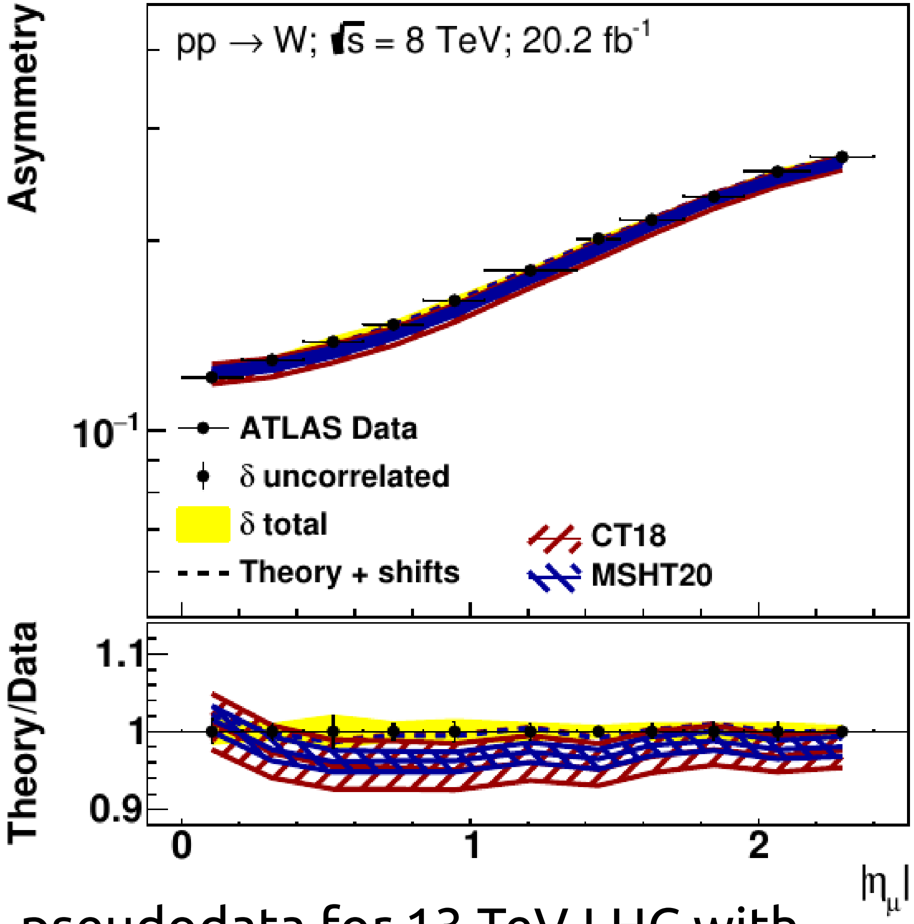

A_W pseudodata for 13 TeV LHC with precision corresponding to integrated luminosities stages:

- 300 fb^{-1} (end of LHC Run-III)
- 3000 fb^{-1} (HL-LHC stage)

Lepton-charge asymmetry

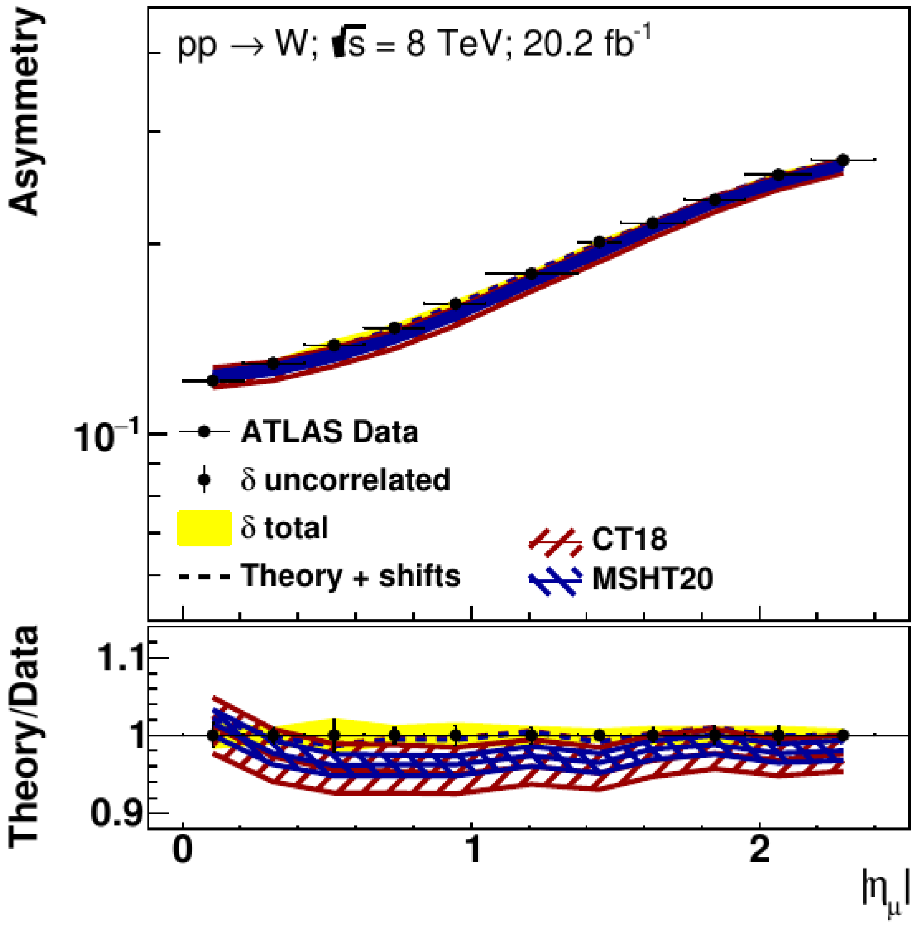

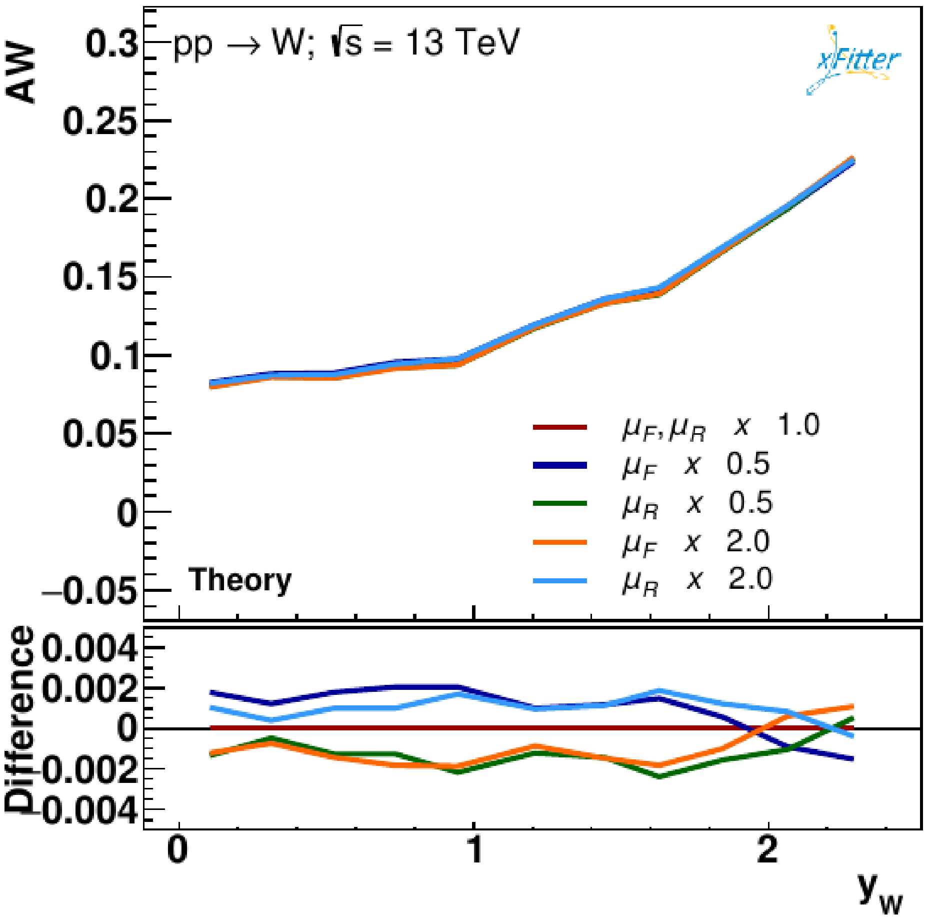

Theory uncertainty from scale variation under control, well below PDF uncertainties.

A_W eigenvector rotation

Assess the single PDF sensitivity on A_W data through eigenvector rotation exercise:

J. Pumplin (2009)

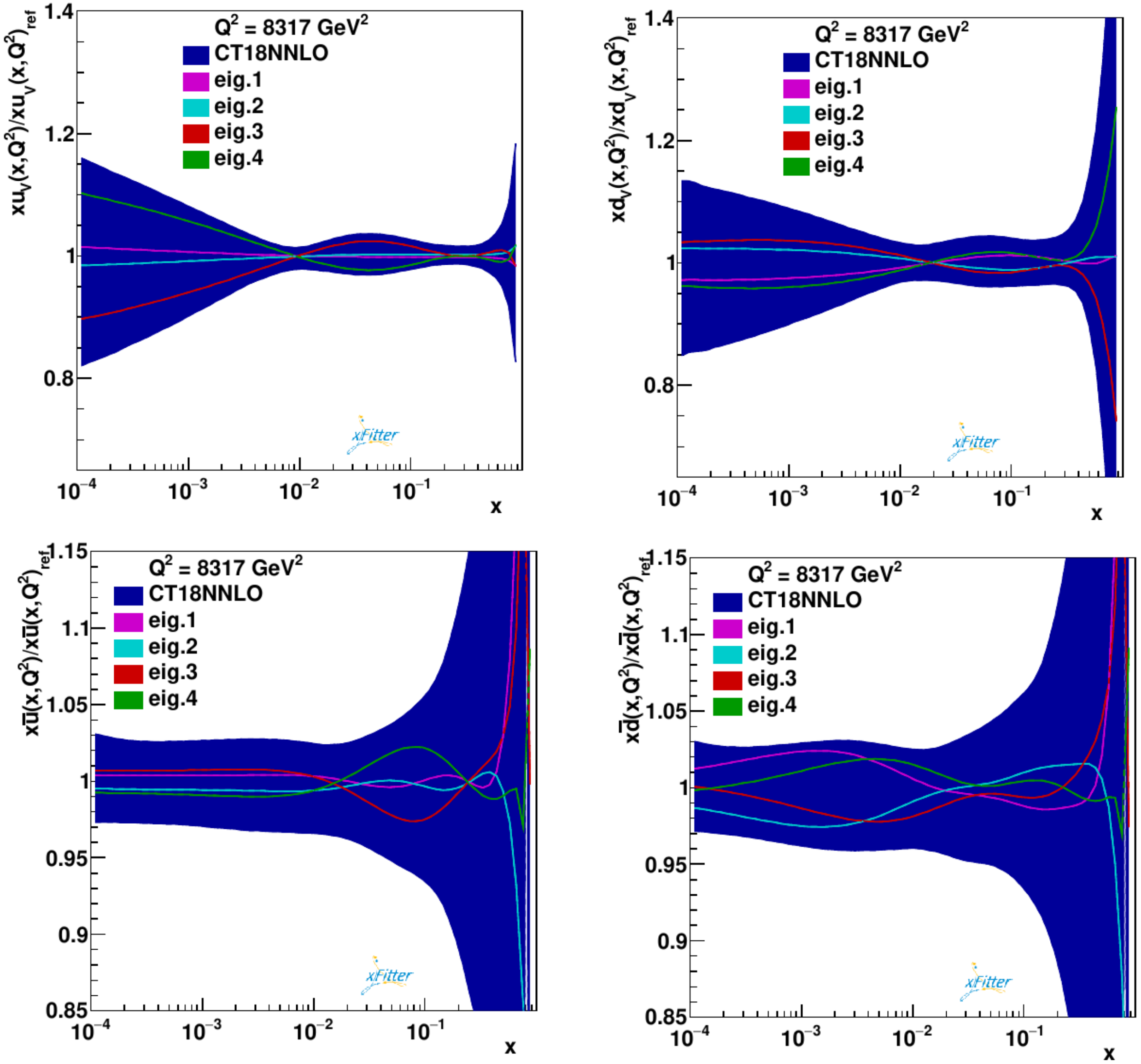

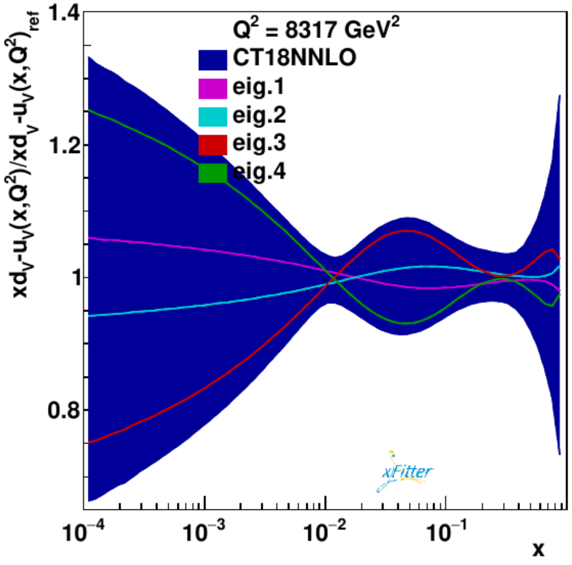

Largest sensitivity on valence quarks, particularly on the combination **(d_V – u_V)**

Complementarity with A_{FB} most sensitive to **(1/3 d_V +2/3 u_V)**

JF, F. Giuli, F. Hautmann, S. Moretti (2021)

Impact on M_W determination

Reduction of PDF uncertainties crucial for SM precision measurements.

Lepton + MET transverse mass spectrum for extraction of M_W

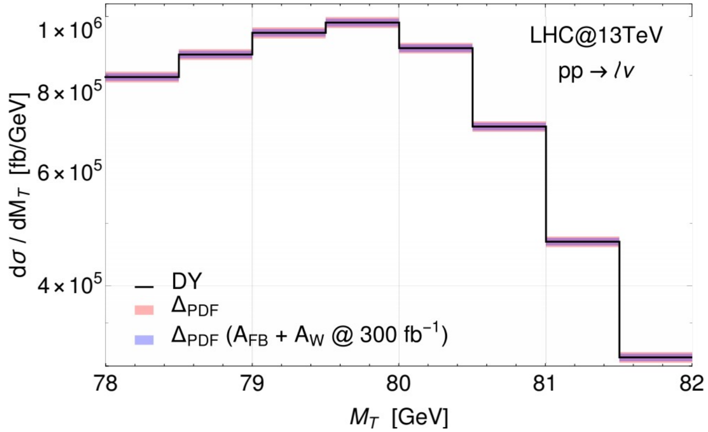

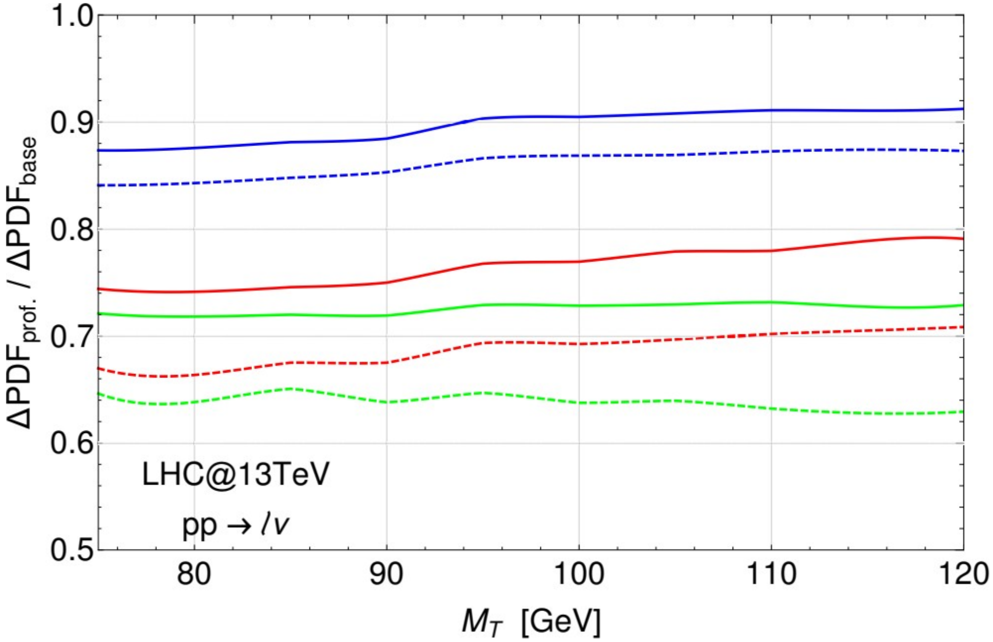

PDF uncertainty before profiling about 1.8%

JF, F. Giuli, F. Hautmann, S. Moretti (2021)

- **A_{FB}** 300 (3000) fb^{-1} data reduces PDF uncertainty ~ 12% (~16%)
- **A_W** 300 (3000) fb^{-1} data reduces PDF uncertainty ~26% (43%)
- Combination of **A_{FB}** and **A_W** 300 (3000) fb^{-1} reduces PDF uncertainty ~28% (~46%)

(REMARK: assessing the improvement on M_W measurement requires a delicate and refined analysis of normalized distribution, where reduction of uncertainty is far more moderate)

Effects on *Z'* searches

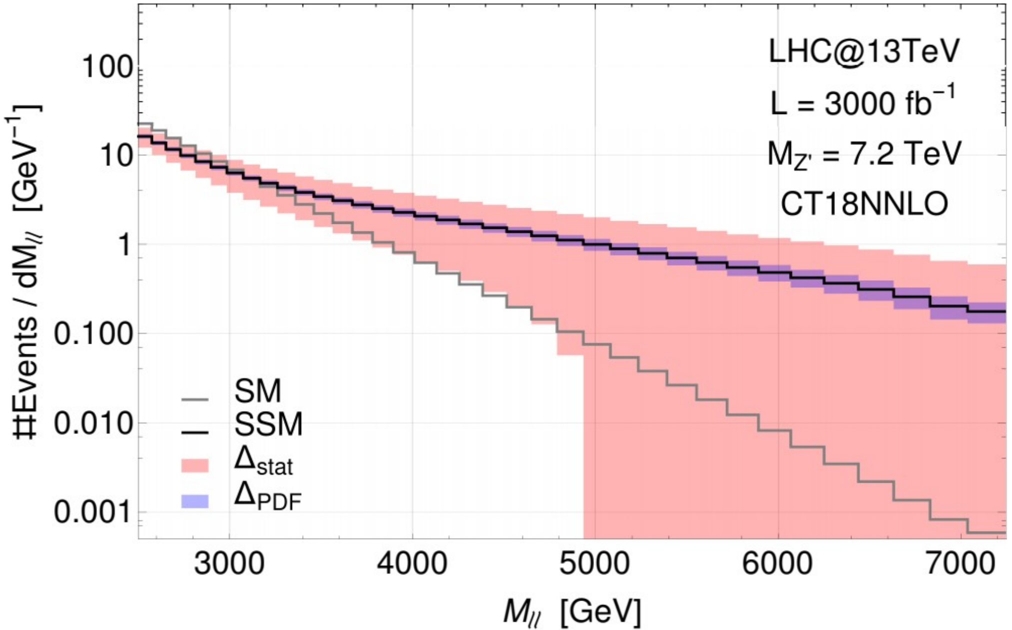

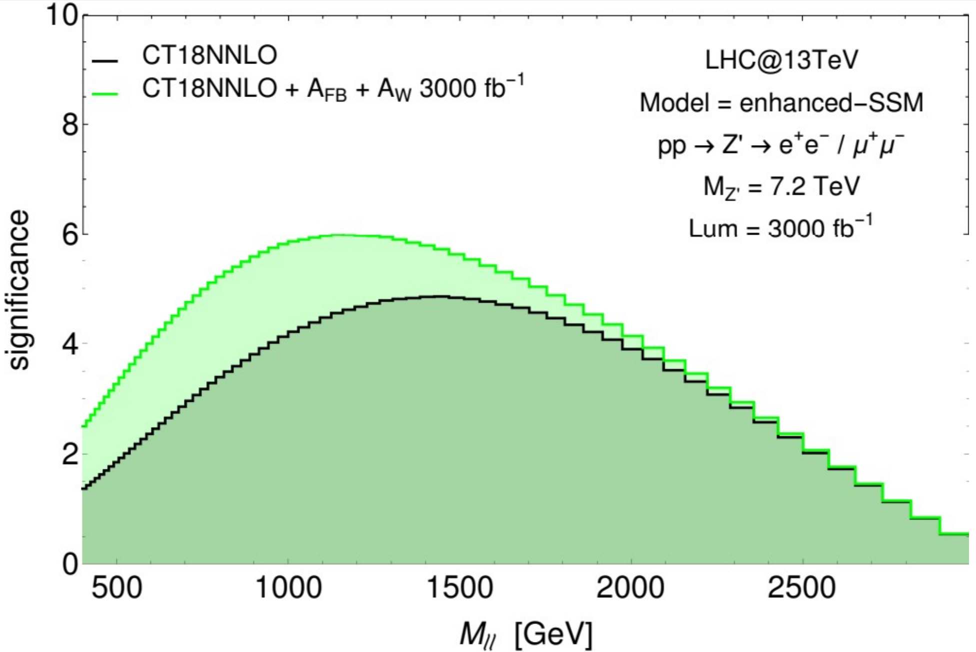

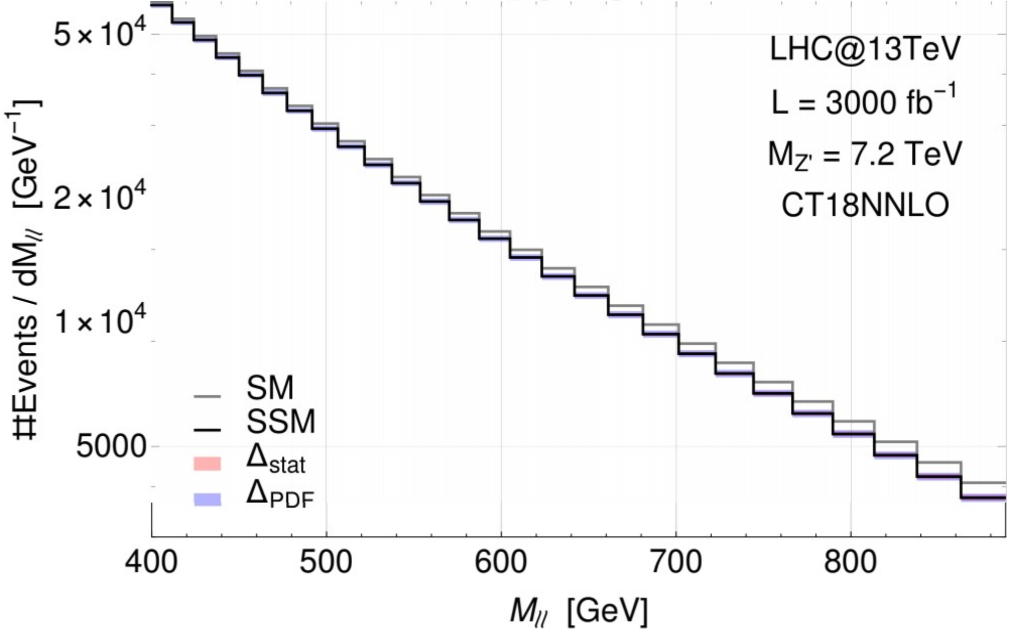

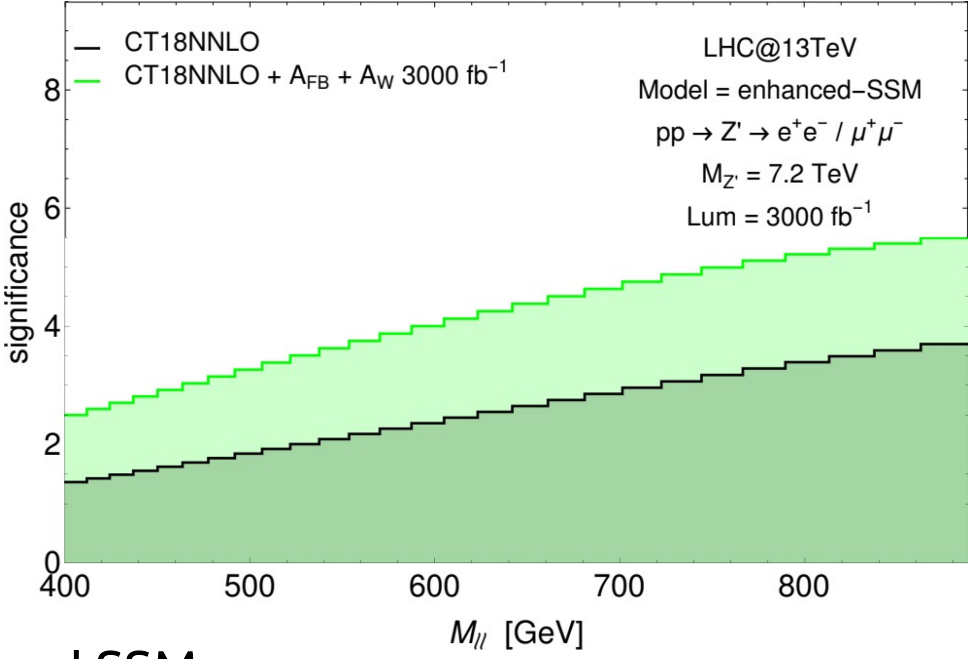

Z' from enhanced SSM

JF, F. Giuli, F. Hautmann, S. Moretti (2021)

Effects on *W'* searches

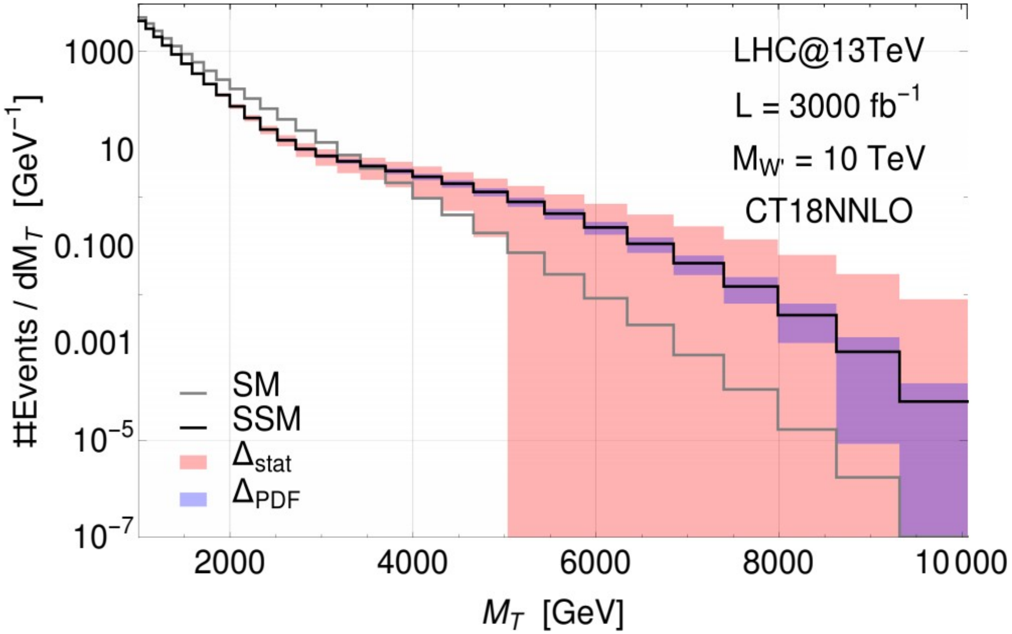

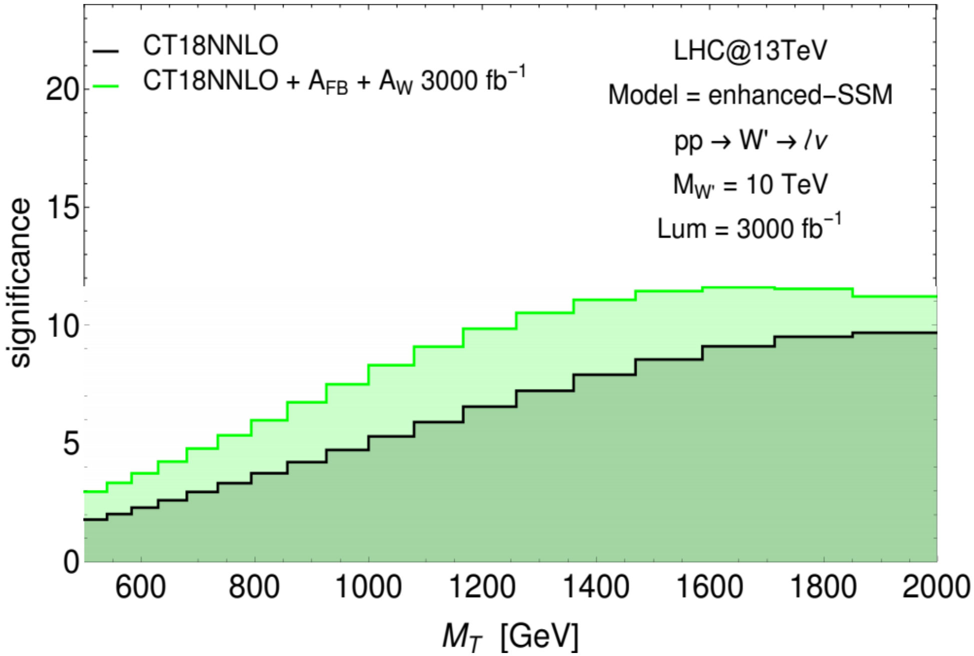

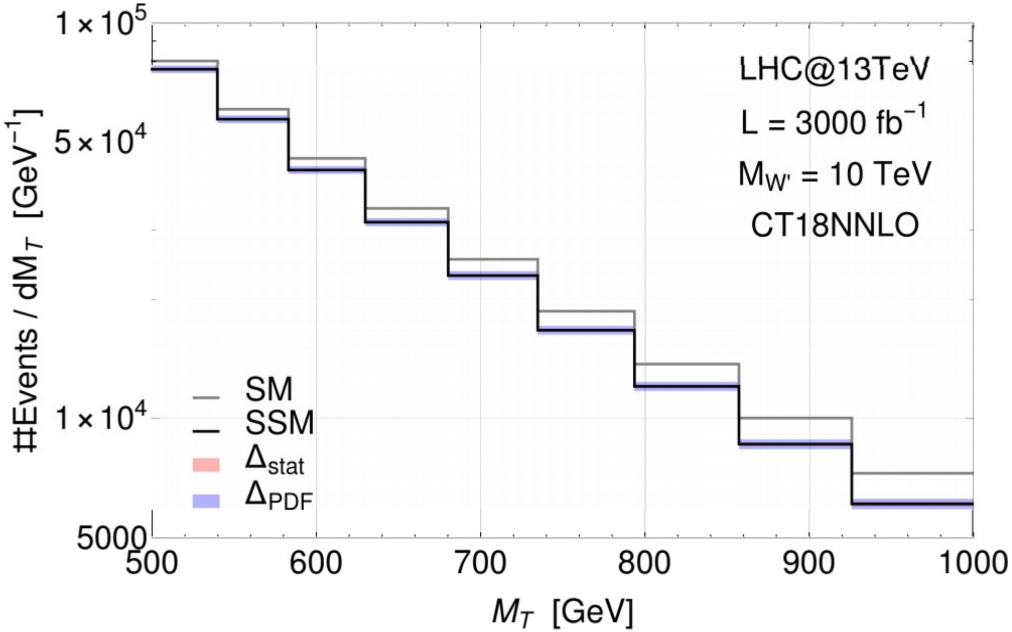

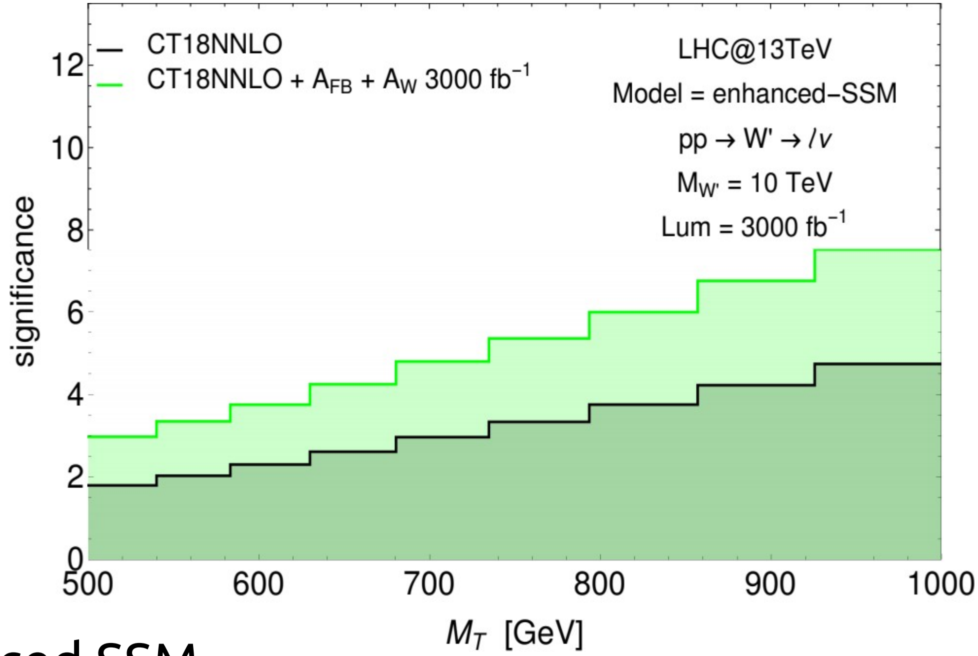

W' from enhanced SSM

JF, F. Giuli, F. Hautmann, S. Moretti (2021)

The angular coeficient A_0

- **A_0** coefficient is parity conserving and sensitive to the flavor singlet PDFs.

- Can be contructed from longitudinal and unpolarized cross sections:

$$A_0(s, M, Y, p_T) = \frac{2d\sigma^{(L)}/dMdYdp_T}{d\sigma/dMdYdp_T}$$

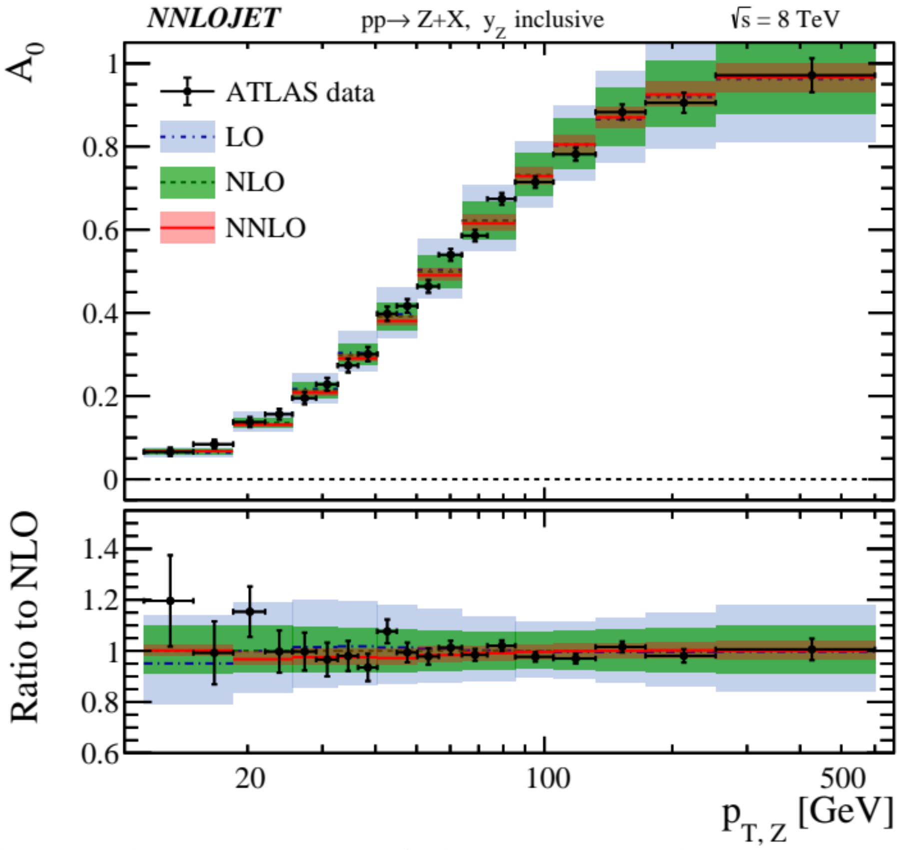

- It has been calculated at NNLO QCD (good convergence of perturbative expansion).

  R. Gauld, et al. (2017)

- NLO EW corrections are small at high p_T^Z.

  R. Frederix, T. Vitos (2020)

PDF set	Total χ^2/d.o.f.
CT18NNLO	59/53
CT18Annlo	44/53
NNPDF31_nnlo_as_0118_hessian	60/53
ABMP16_5_nnlo	62/53
MSHT20nnlo_as118	59/53
HERAPDF20_NNLO_EIG	60/53

Validation of the implementation of the observable in xFitter:

- 3 rapidity bins
- p_T > 11.4 GeV
- Predictions at order α_s^2 from MadGraph5_aMC@NLO
- Covariance matrix of experimental uncertainties included

Good description of the data from modern PDFs

The angular coeficient A_0

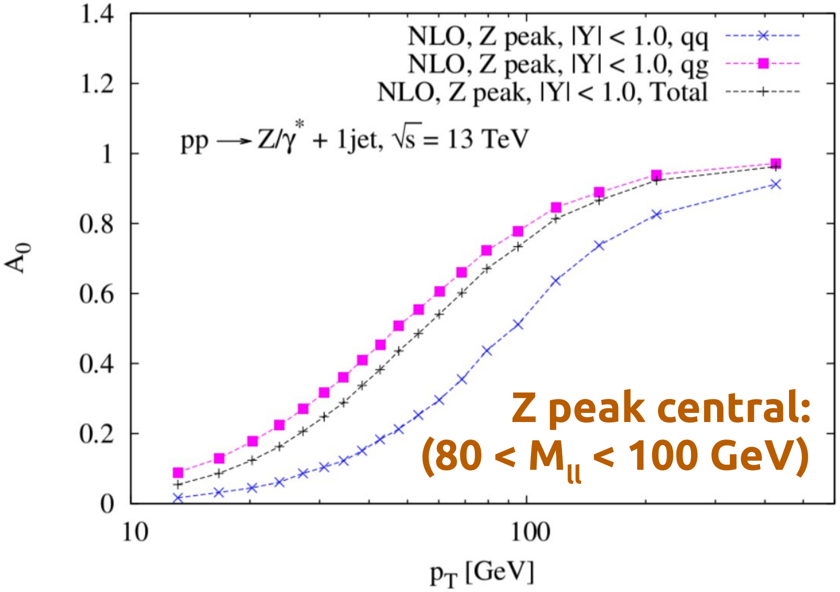

Z peak central:
(80 < M_{ll} < 100 GeV)

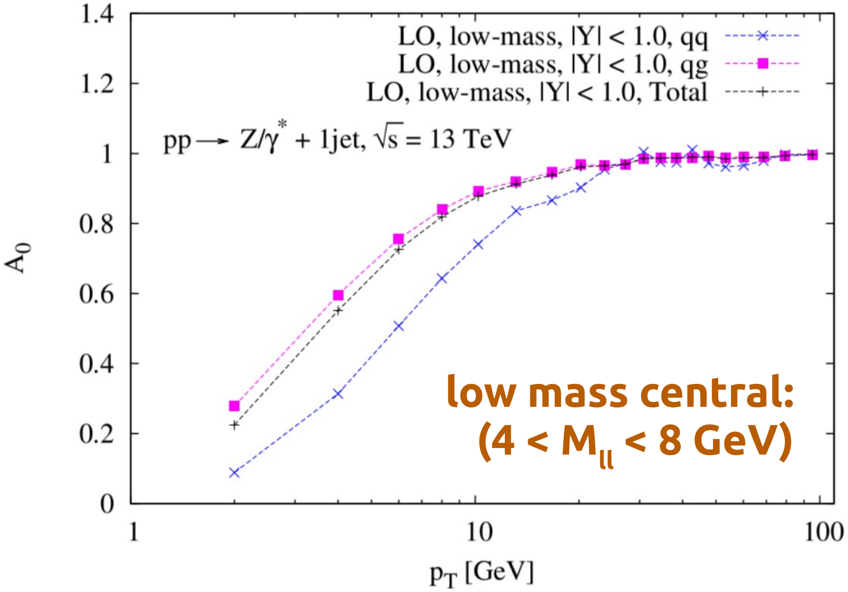

low mass central:
(4 < M_{ll} < 8 GeV)

- A_0 pseudodata evaluated in different invariant mass regions and rapidity ranges.
- Contributions from both $q\bar{q}$ and qg channels.
- Largest sensitivity on PDFs in the region at the saddle point ($\partial^2 A_0/\partial p_T^2 = 0$).
- Pseudodata generated for 13 TeV c.o.m. energy and projected statistical uncertainties for **300** and **3000 fb^{-1}** luminosity.
- 0.1% systematic uncertainty on leptons momentum scale.

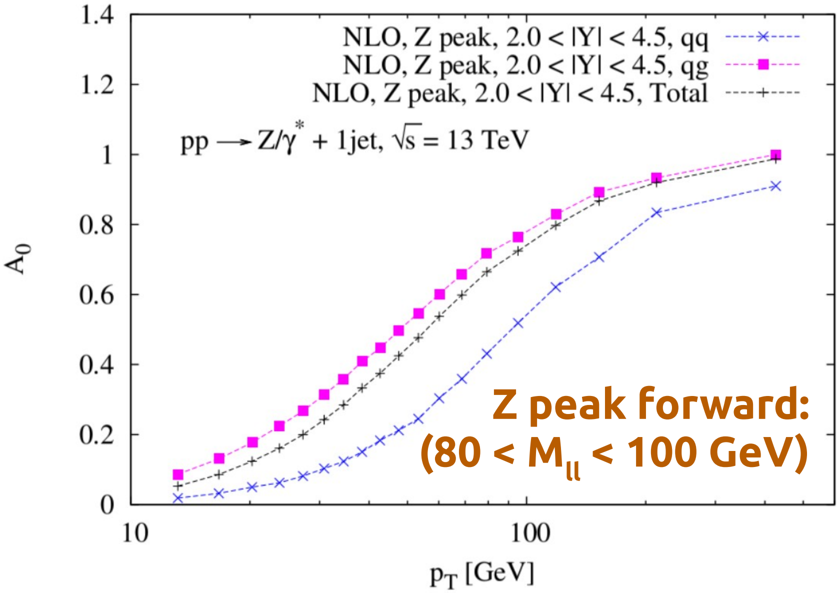

Z peak forward:
(80 < M_{ll} < 100 GeV)

JF, S. Amoroso, et al. (2021)

A_0 @ Z peak

- Profiling of xg, xg/Σ, $x\bar{u}$, $x\bar{d}$
- Largest constrains in the region $10^{-3} < x < 10^{-1}$
- Largest impact from 300 fb^{-1} data, but 3000 fb^{-1} data can further constrains $x\bar{u}$, $x\bar{d}$
- Results are stable against variations of ren/fact scales

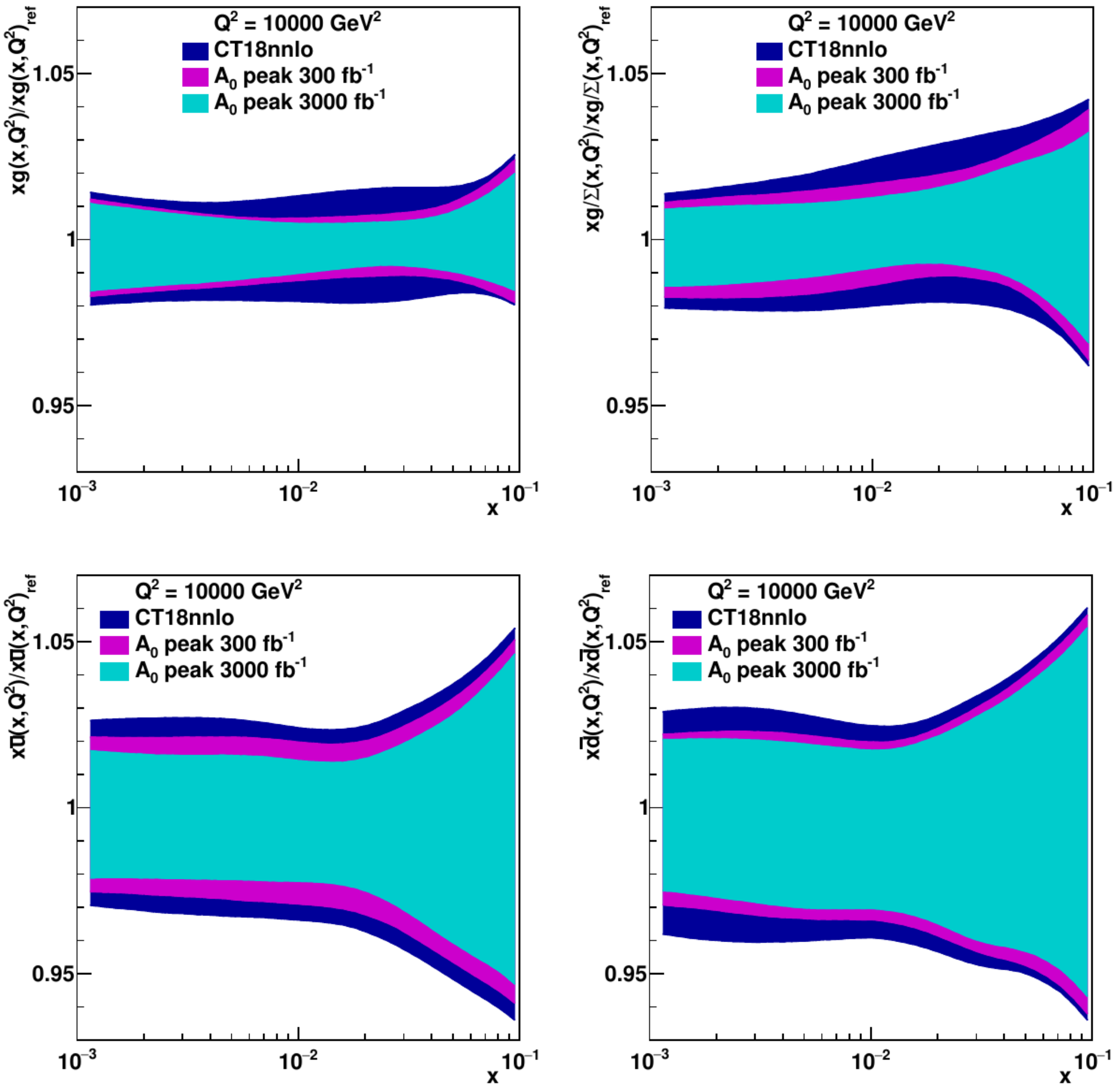

JF, S. Amoroso, et al. (2021)

A_0 @ low mass and high rapidity

- Profiling using low invariant mass data
  ($4 < M_{ll} < 8$ GeV)
  - Sensitive to gluon PDF at low-x, $x < 10^{-3}$
  - Possibly useful for TMD PDFs determination

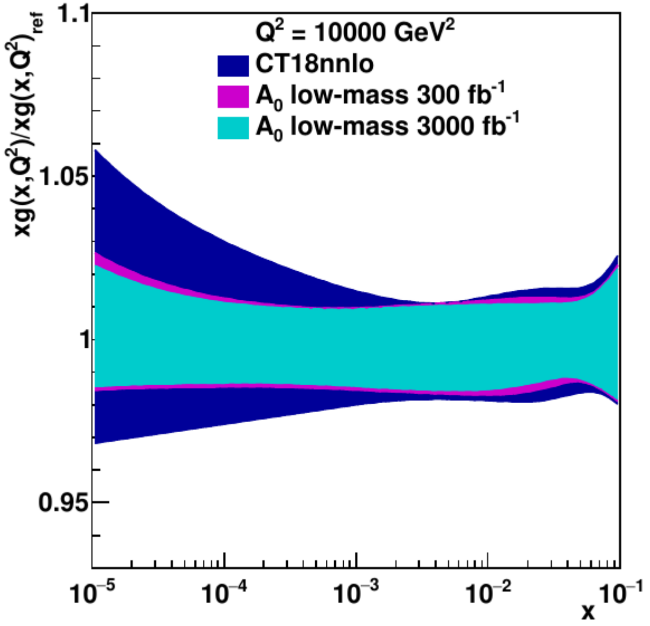

- Profiling using forward rapidity region (LHCb reach):
  ($2.0 < y_{ll} < 4.5$)
  - Improvements in sea quark PDFs at intermediate x, $x \sim 10^{-3}$

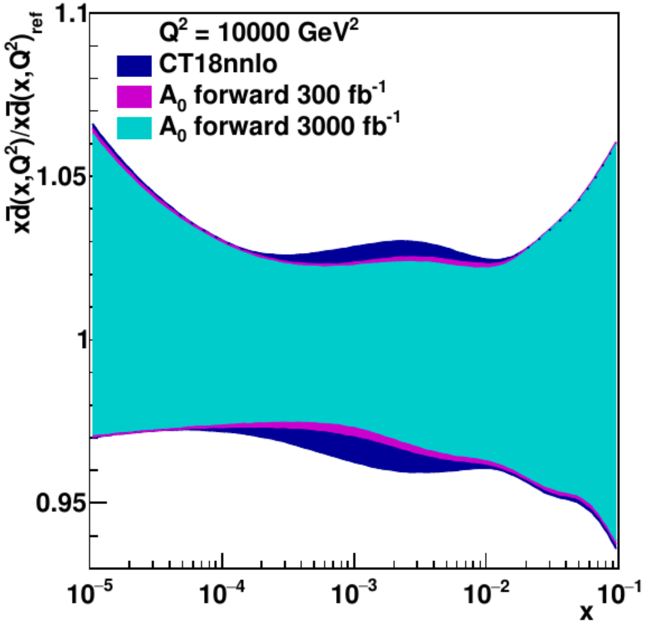

JF, S. Amoroso, et al. (2021)

Impact of A_0 on Higgs cross section

- Gluon-gluon luminosity as function of M_X computed at NLO QCD with MCFM.
- PDF uncertainties are reduced by 30%-40% in the Run-III scenario and about 50% in the HL-LHC scenario in the region **$100 < M_X < 200$ GeV** .

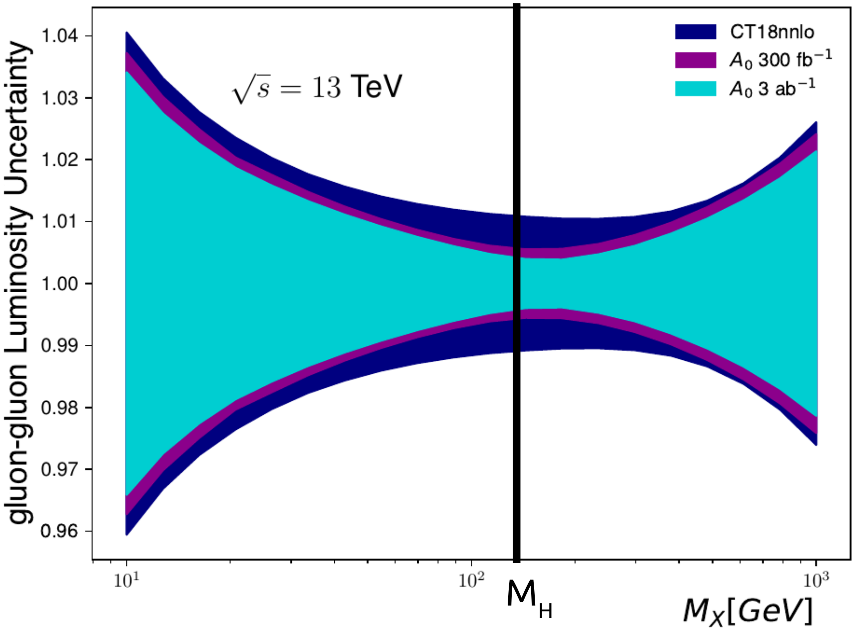

- Reduction of uncertainties concentrated in the central rapidity region **$|y_H| < 2.0$** .

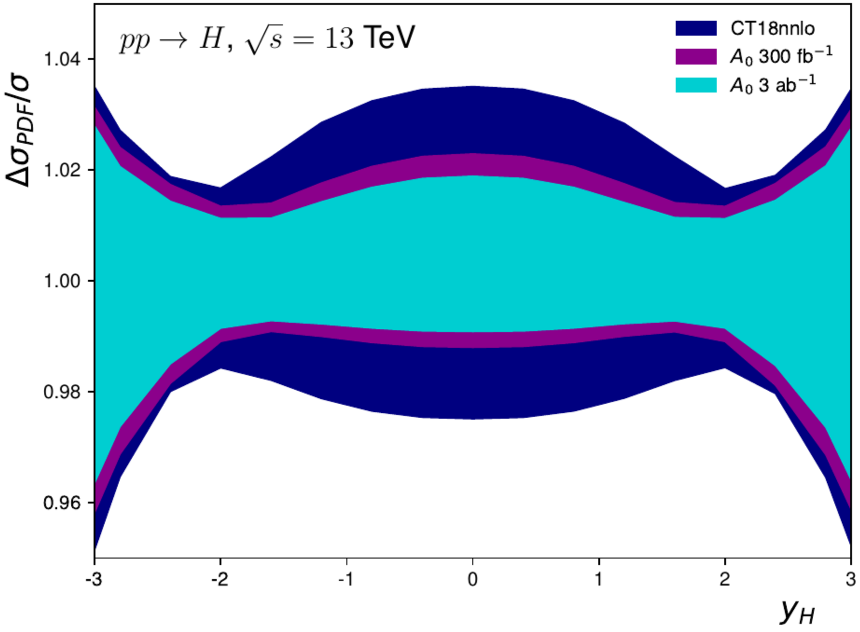

JF, S. Amoroso, et al. (2021)

Impact of A_0 on Higgs cross section

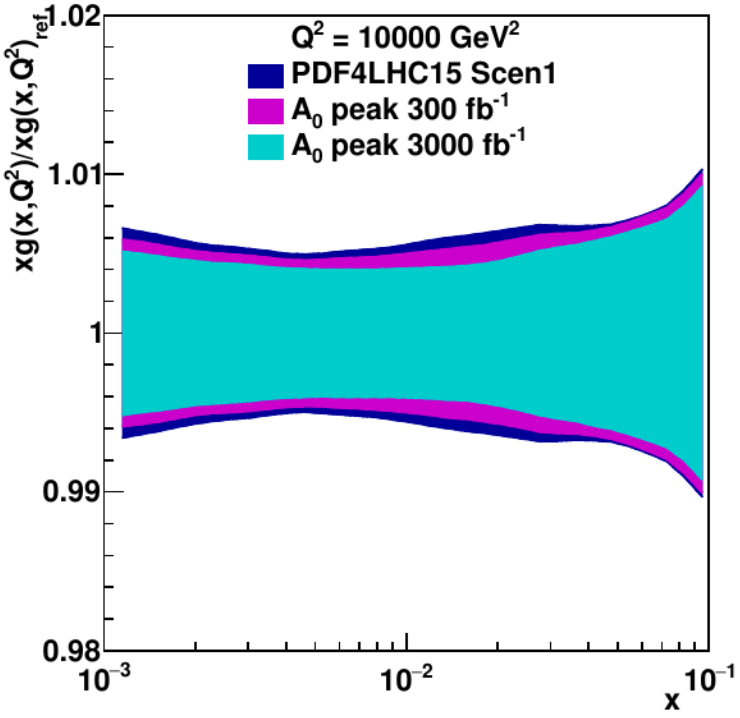

- Profiling projected PDFs based on complete HL-LHC data sample (include jet and top measurements). EPJC 78 (2018) 11

- Further reduction of uncertainty can be obtained.

- In ggF computed at N^{3}LO, the reduction of uncertainty is visible <u>in all modern and projected PDF sets</u>.

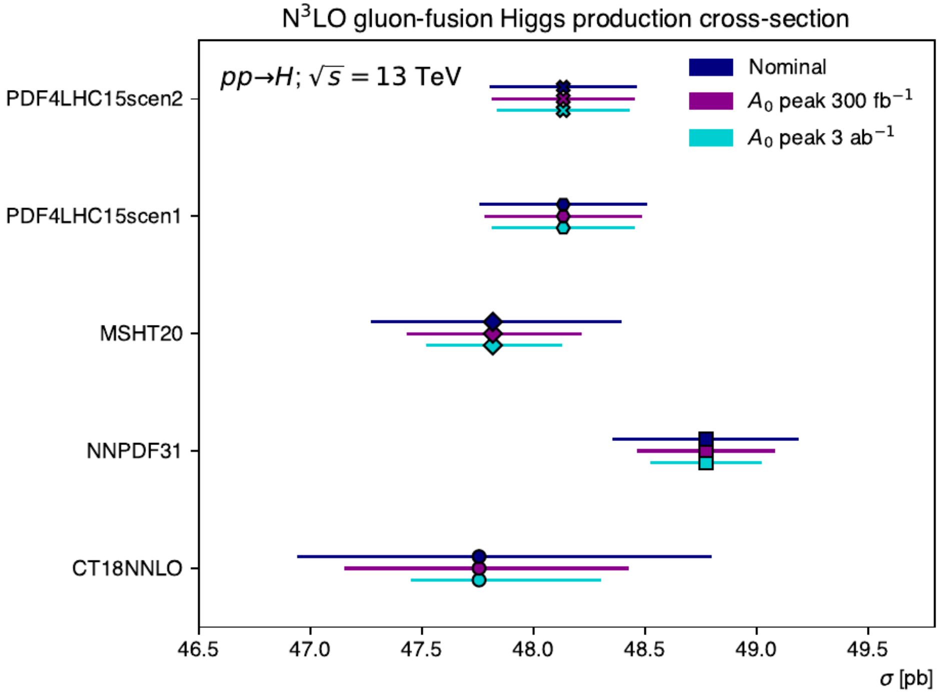

JF, S. Amoroso, et al. (2021)

PDFs prospects

Each PDF set comes with its error estimation:

JF, E. Accomando, F. Hautmann, S. Moretti (2018)

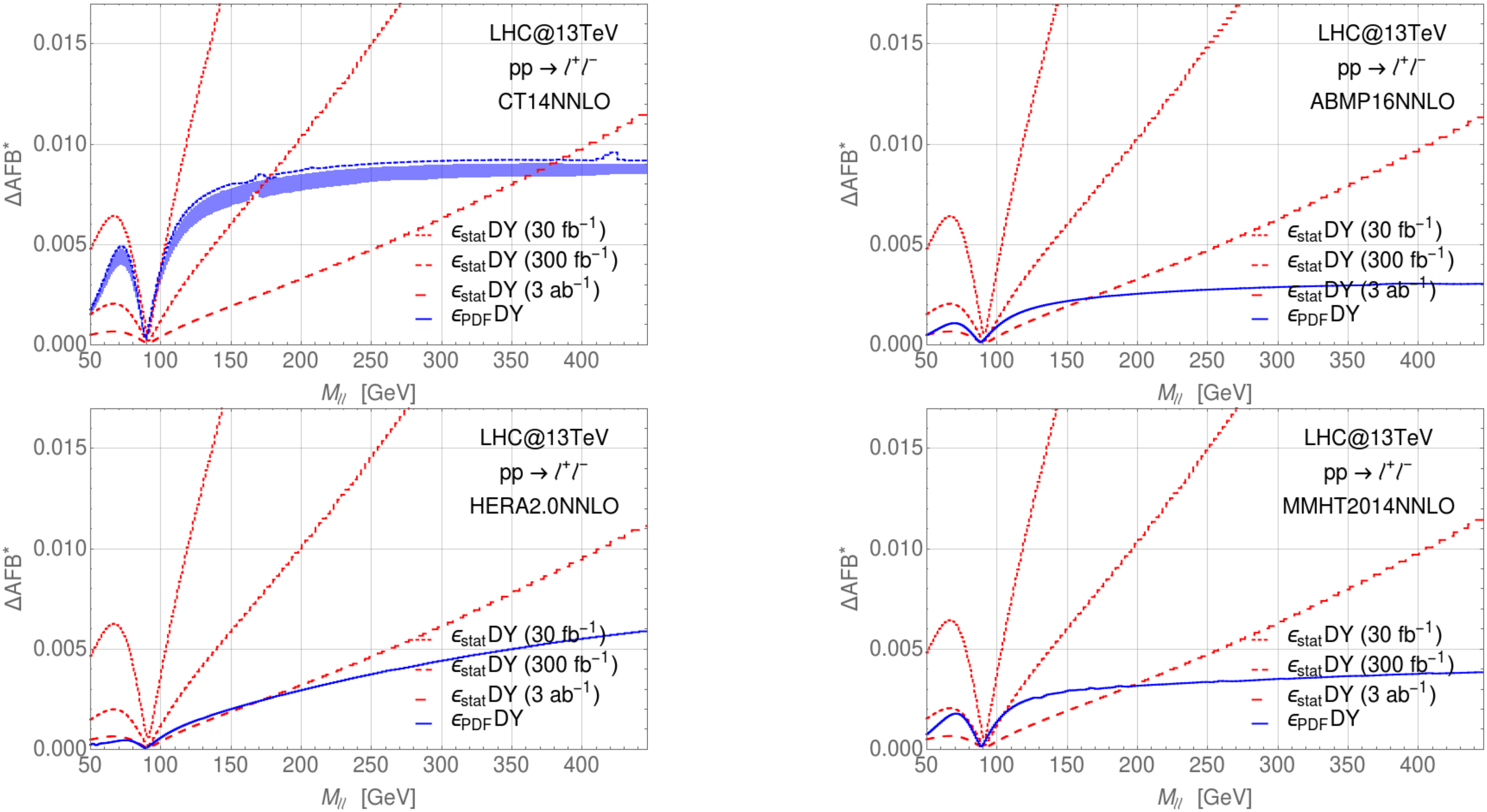

Each PDF fit would benefit from the inclusion of the AFB*.

Parton Luminosities

JF, E. Accomando, F. Hautmann, S. Moretti (2018)

Imposing a high rapidity cut on the final state system we select processes arising from extreme Bjorken x regions.

With *|Y| = 4.5* at the *Z* pole we are exploring:

$$\begin{cases} x_1 \simeq 6\times10^{-1} \\ x_2 \simeq 8\times10^{-5} \end{cases}$$

$$x_{1,2} = \frac{\sqrt{\hat{s}}}{\sqrt{s}} e^{\pm|Y|}$$

(likely high-*x* valence quarks, low-*x* sea anti-quarks)

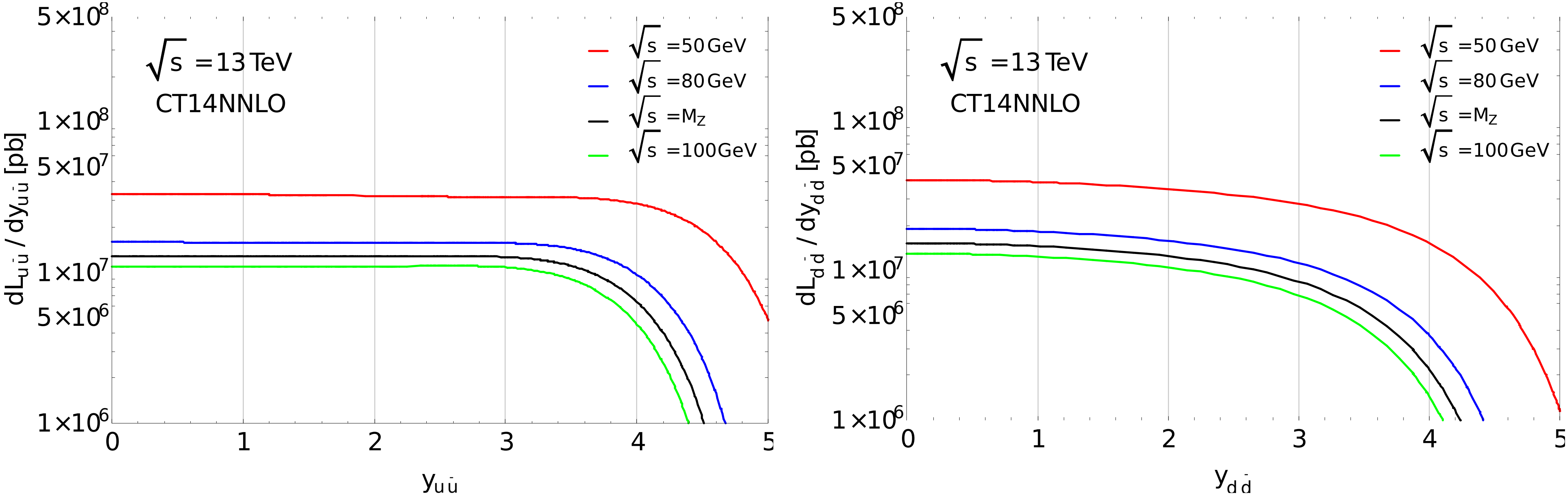

Processes initiated by $d\bar{d}$ interaction are more suppressed than $u\bar{u}$ initiated processes

Parton Luminosities Ratio

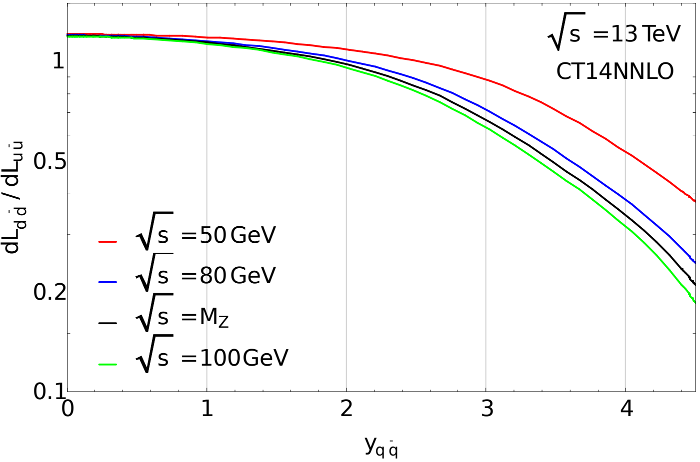

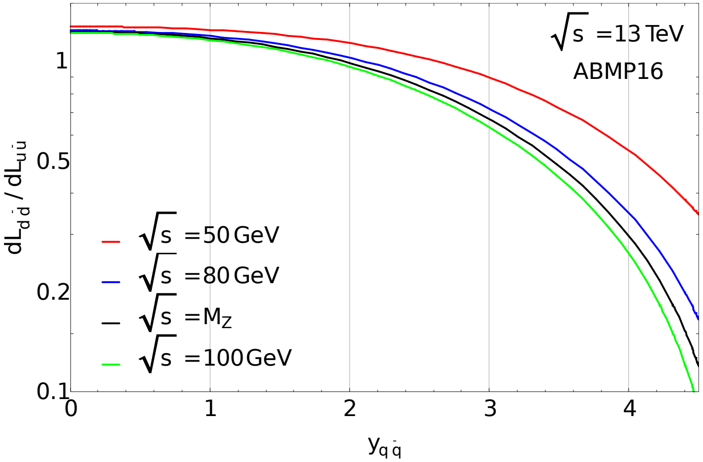

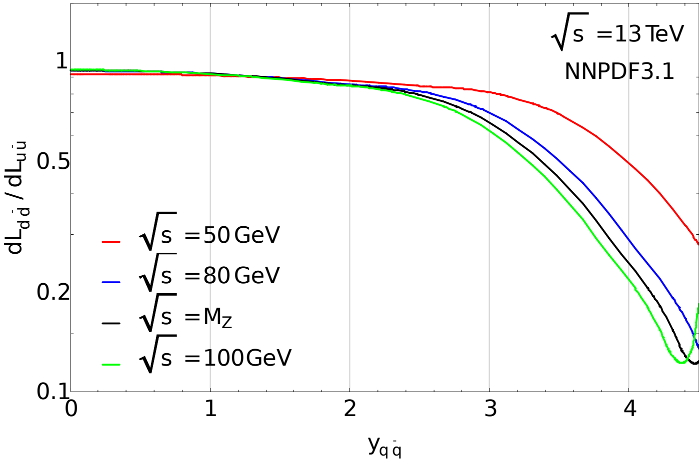

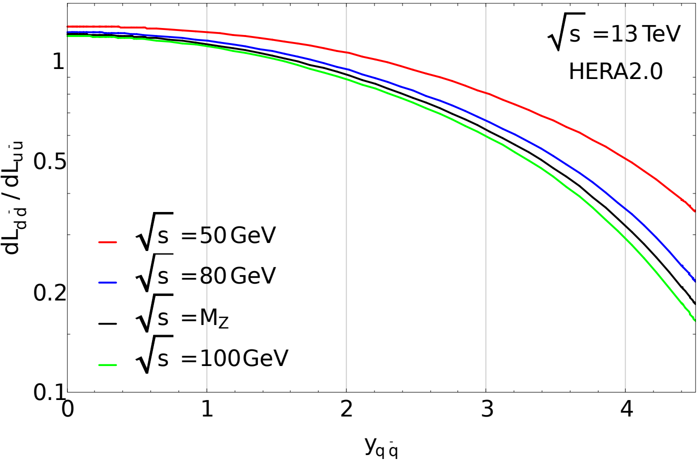

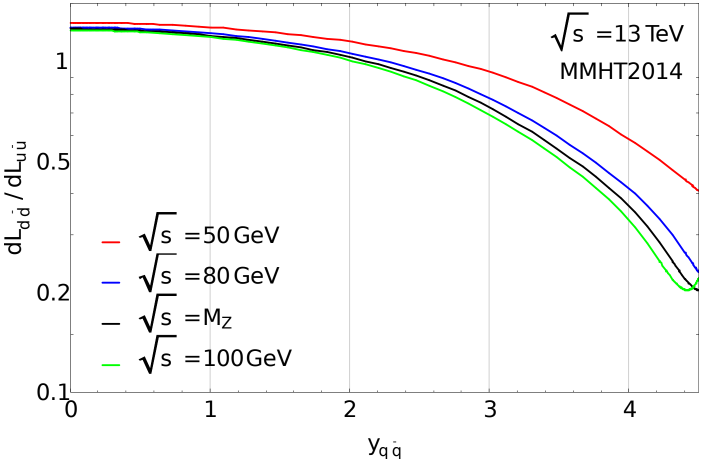

Each PDF set predicts a different partonic content

JF, E. Accomando, F. Hautmann, S. Moretti (2018)

A sufficiently high rapidity cut suppresses the contribution from $d\bar{d}$ interaction and gives us a direct handle on u and $\bar{u}$ PDFs.

Selecting *|Y| = 4.5* at the *Z* pole we have an overall contribution from $d\bar{d}$ initiated processes of:

CT14: 21%

ABMP: 12%

NNPDF: 12%

HERA: 18%

MMHT: 20%

Parton Luminosities Ratio

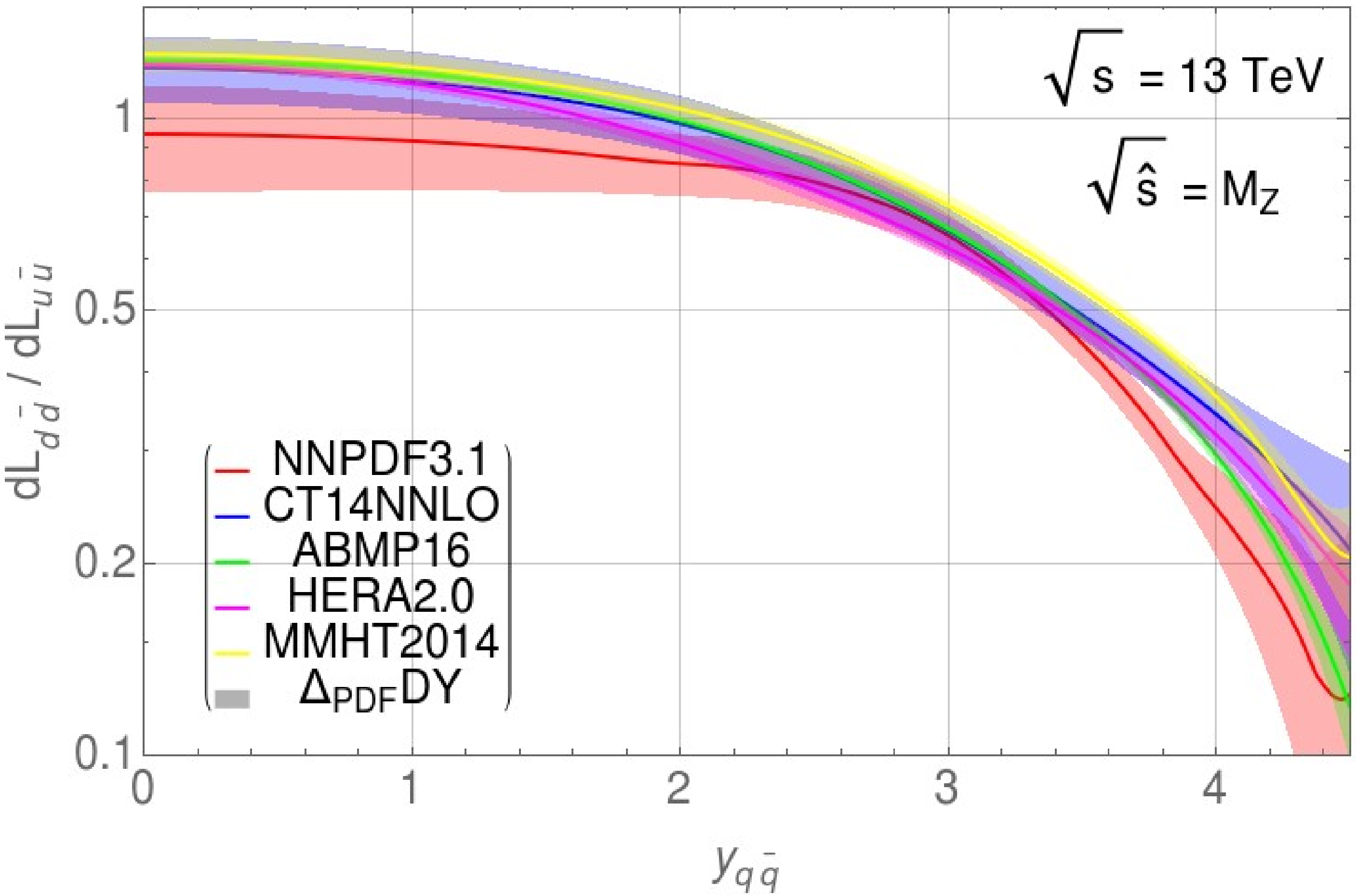

Selecting *|Y| = 4.5* on the *Z* pole we have an overall contribution from $d\bar{d}$ initiated processes of:

NNPDF: 2% - 23% **CT14:** 13% - 29% **ABMP:** 10% - 14% **HERA:** 14% - 23% **MMHT:** 16% - 25%

JF, E. Accomando, F. Hautmann, S. Moretti (2018)

Forward / Backward

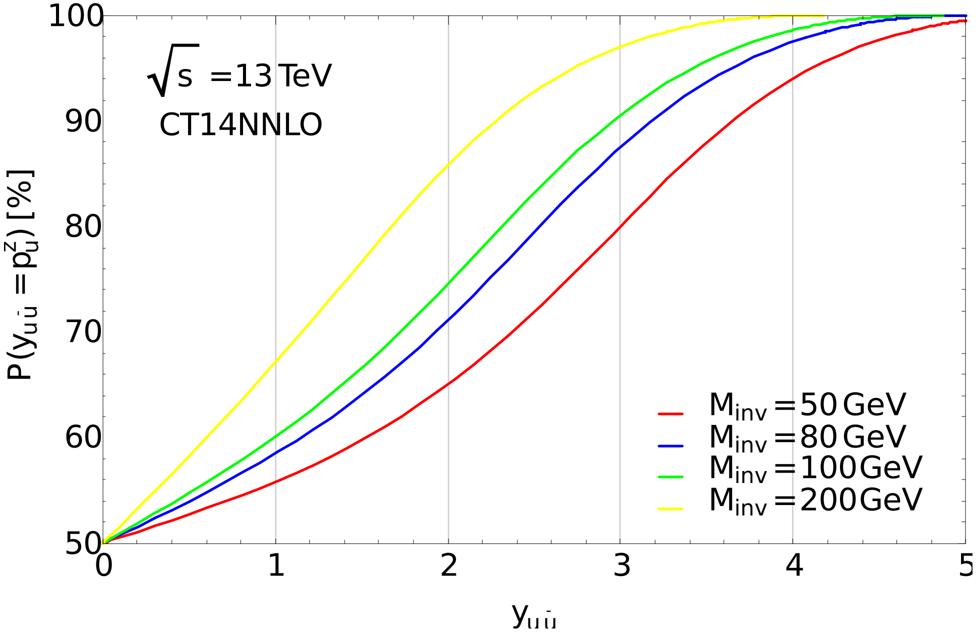

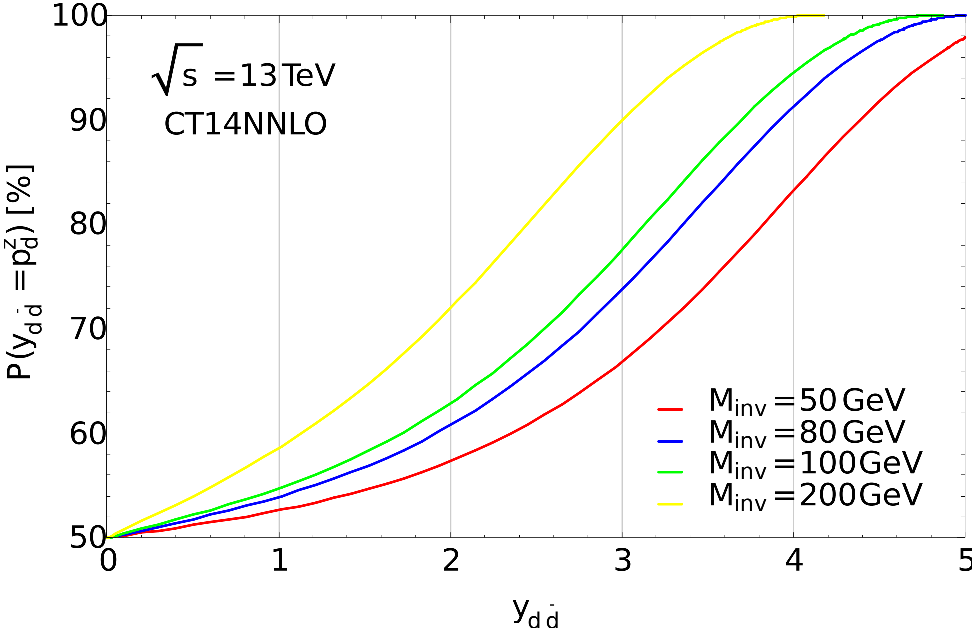

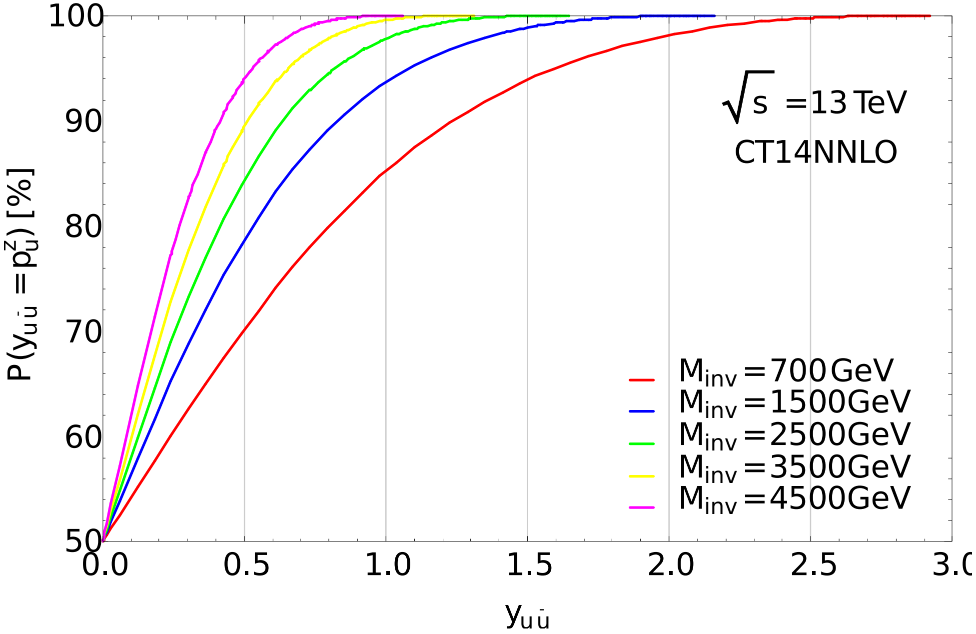

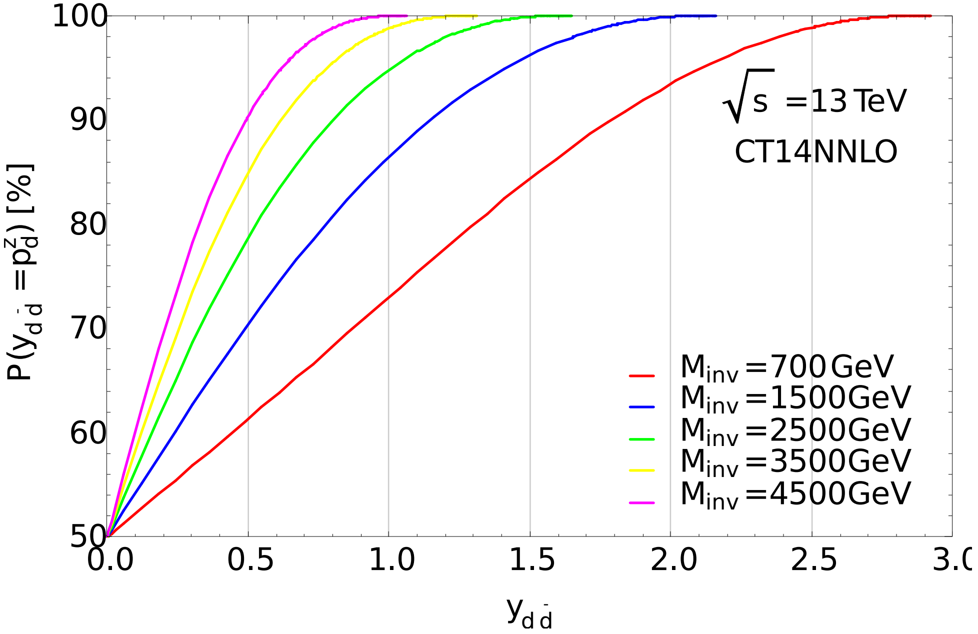

The probability of the direction of the boost matching the direction of the incoming quark grows with the rapidity cut and with the invariant mass, and it is higher for the *up* quarks

High rapidity measurements

Enhancing the rapidity cut we tend to the “true” AFB.

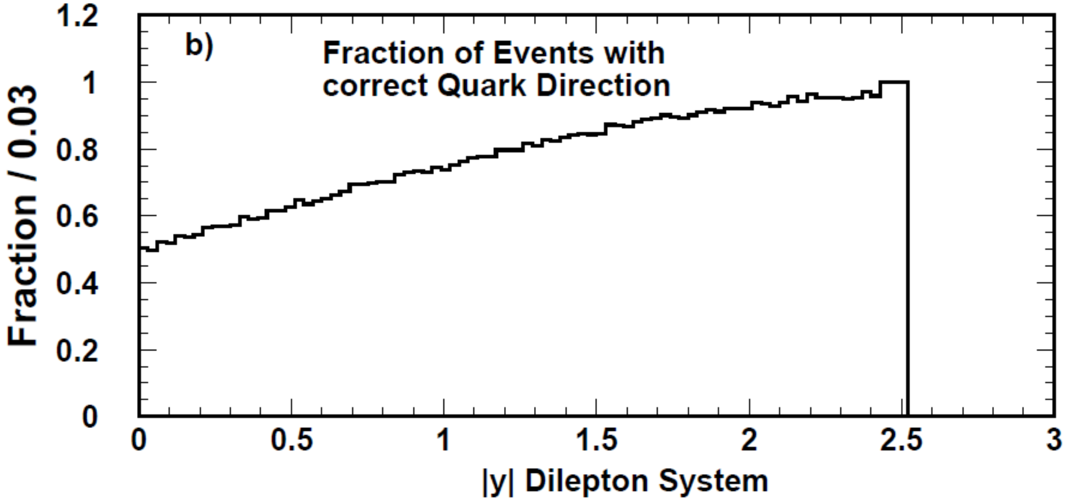

M. Dittmar, Phys.Rev.D55:161-166 (1997)

We are more likely to pick up the direction of the incoming quark (more energetic than the anti-quark).

The partonic luminosity of the down quarks is suppressed.

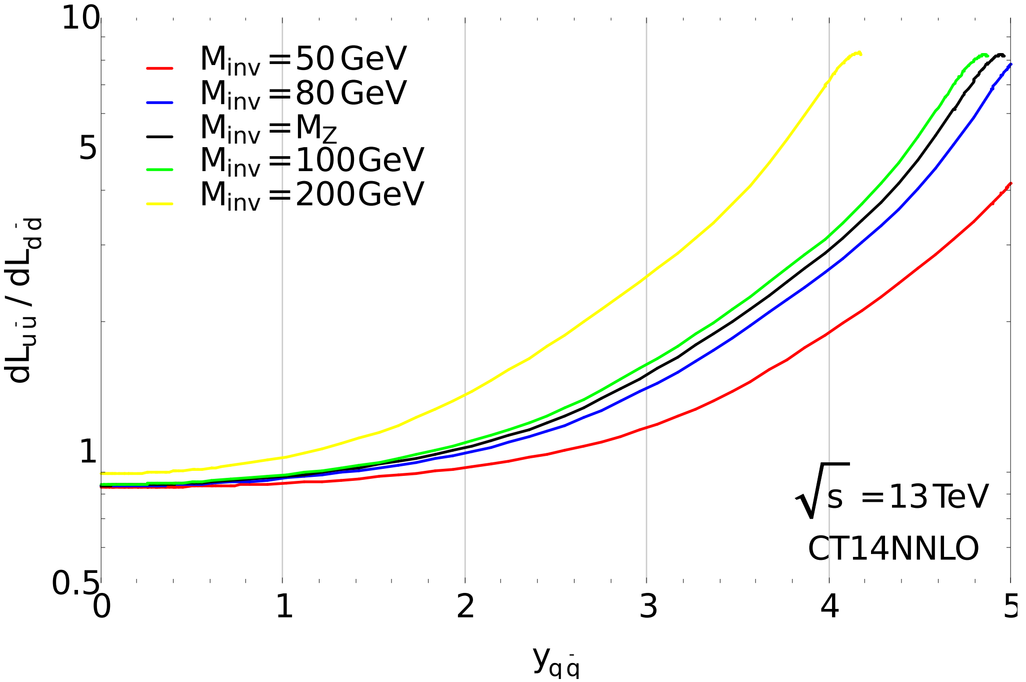

The AFB* in the high rapidity limit is produced by the *$u\bar{u}$* interaction.

For *$|Y| > 4.5$* the down quarks contribution to the AFB* is ~ 20% at the Z pole (CT14NNLO prediction).

We have a direct observation on the *up* quarks PDF in the high-*x* region and a on the *anti-up* quarks in the low-*x* region.

Comparing PDF sets

AFB* measurements can be used to distinguish between different PDFs parametrizations.

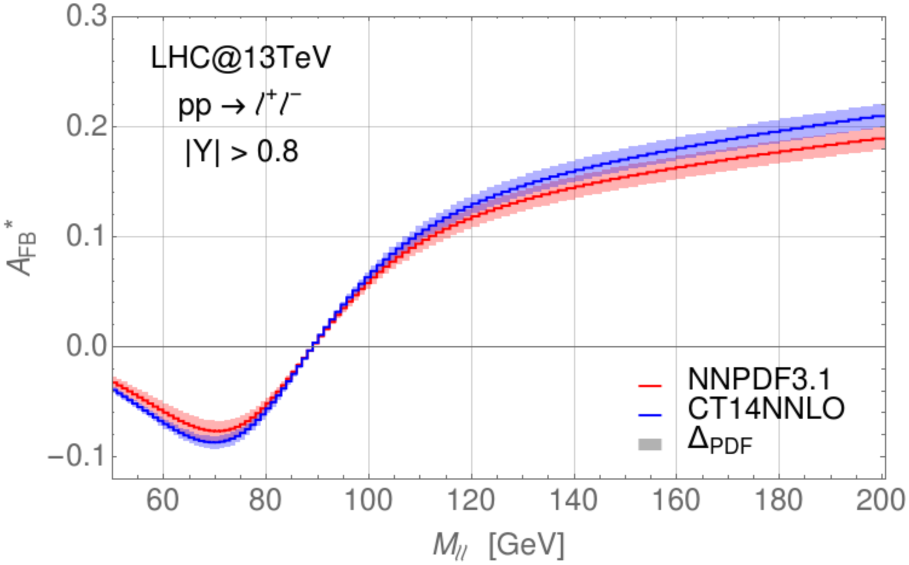

Statistics allows precise measurements

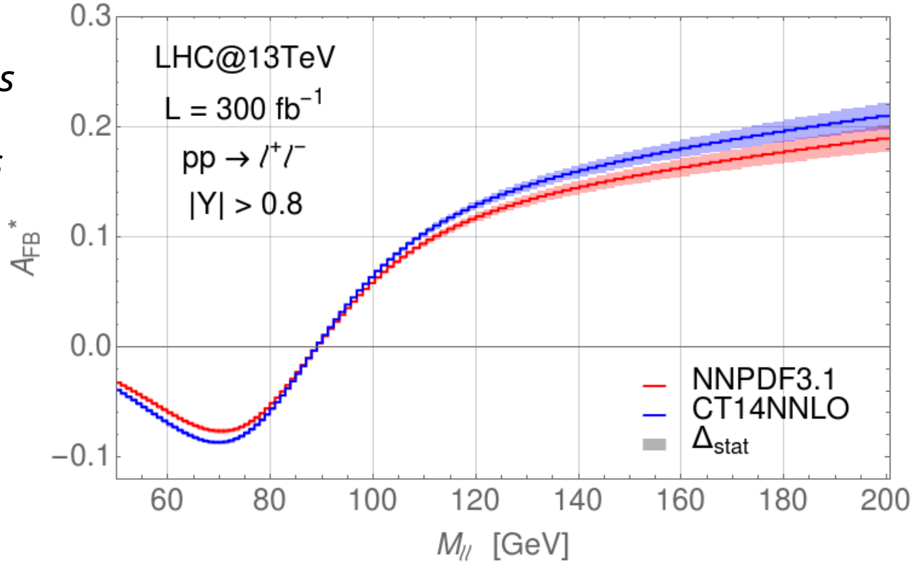

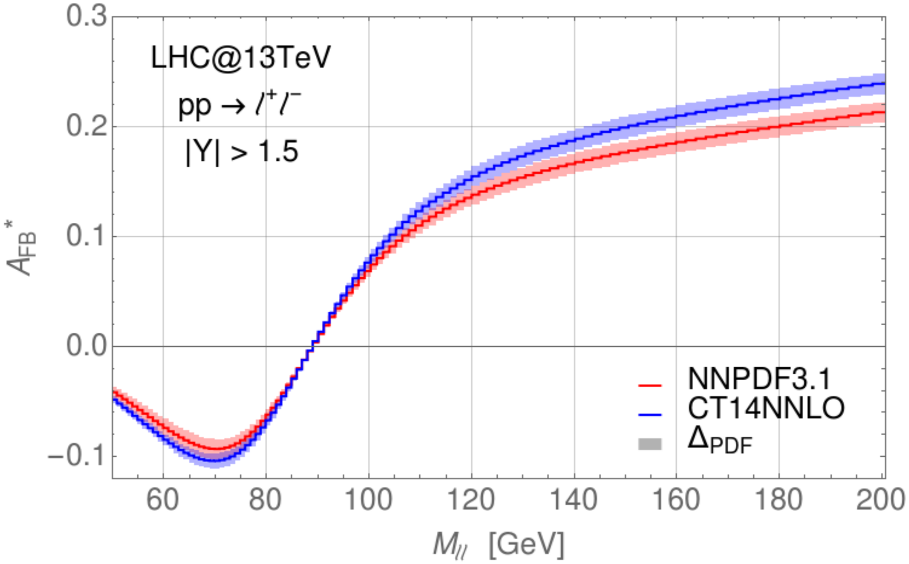

Systematics are under control

(and from what said before they can be further improved)

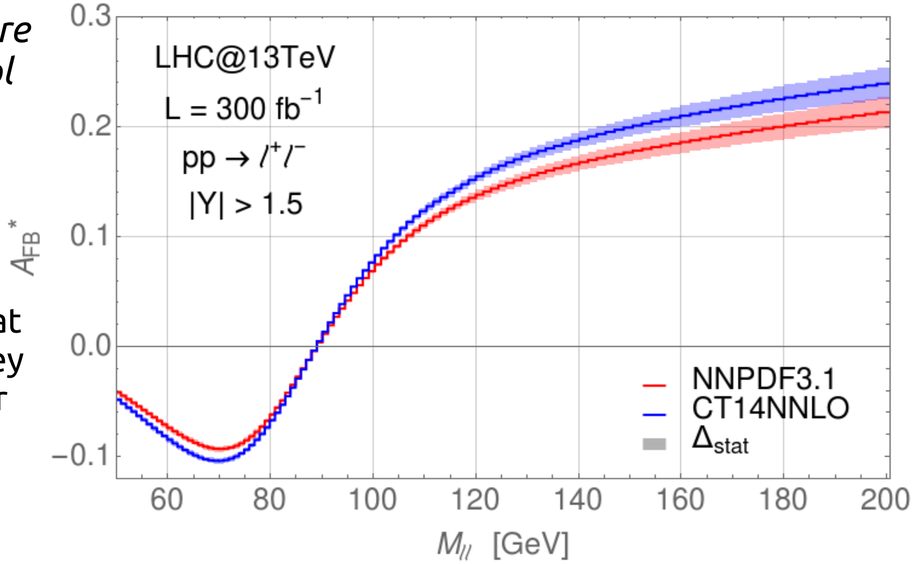

High rapidity cuts enhance the differences between PDF sets.

Comparing PDF sets

AFB* measurements can be used to distinguish between different PDFs parametrizations.

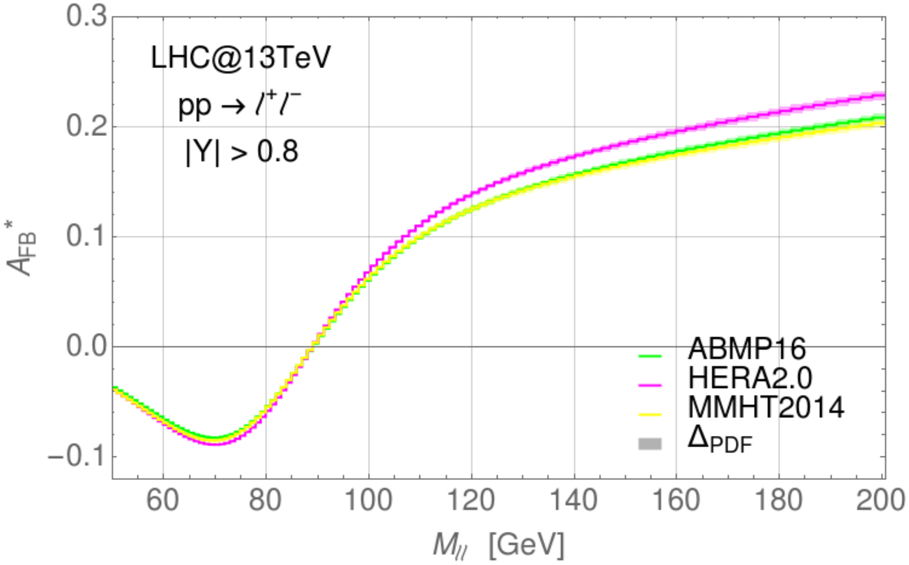

Statistics allows precise measurements

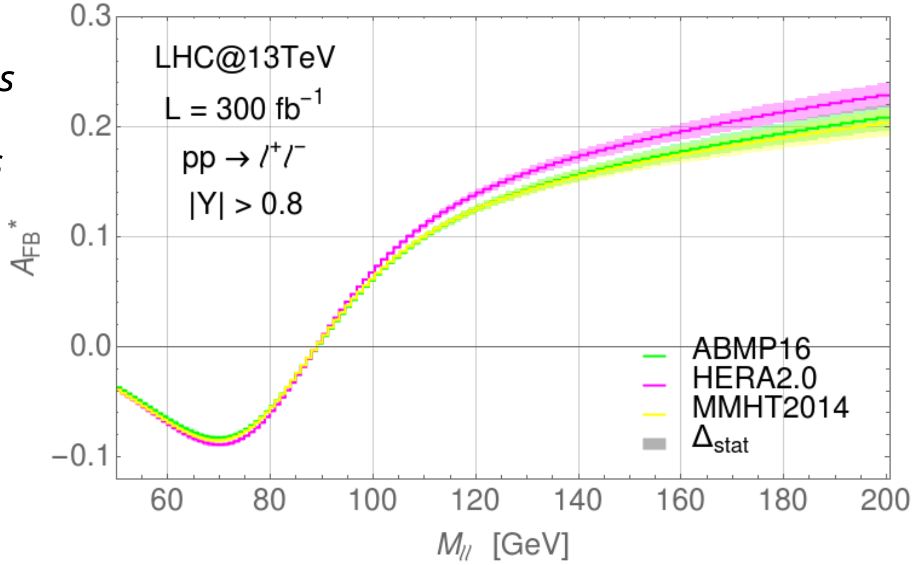

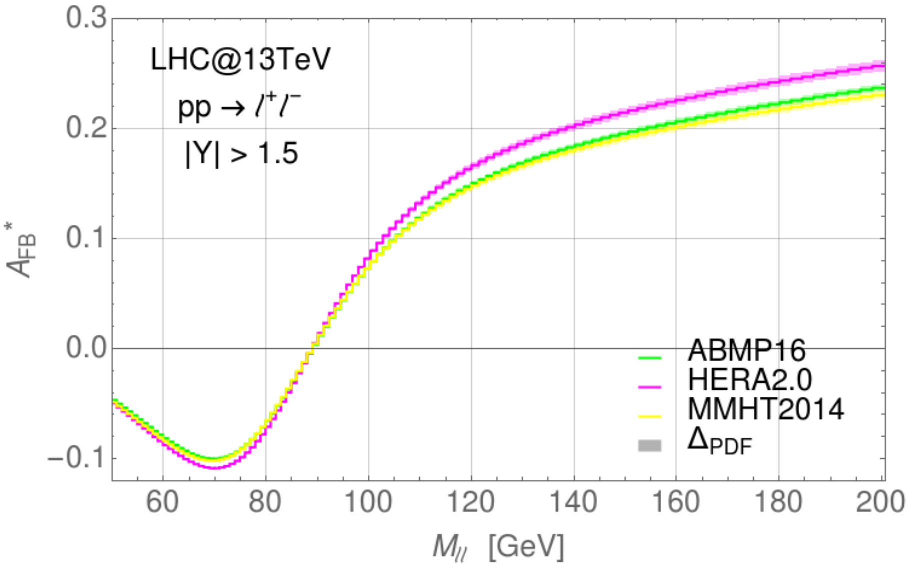

Systematics are under control

(and from what said before they can be further improved)

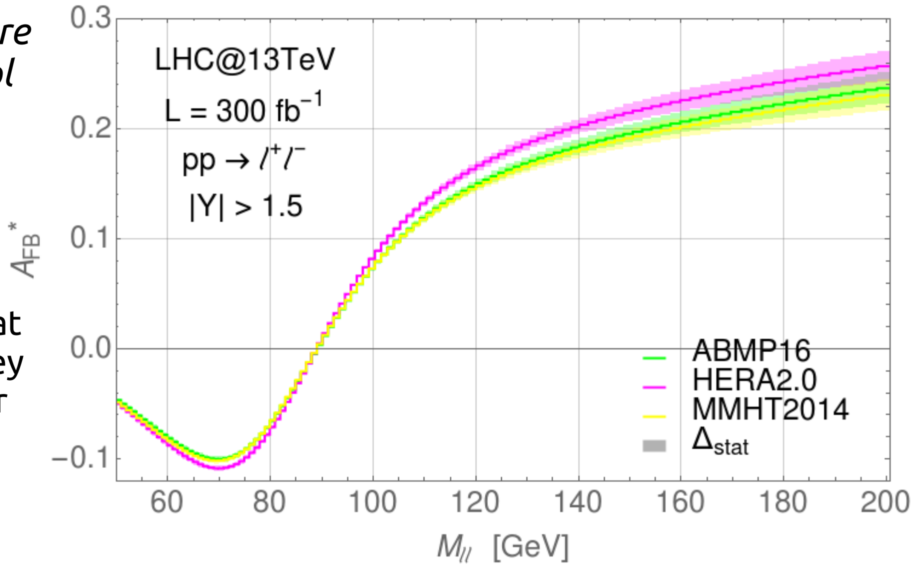

High rapidity cuts enhance the differences between PDF sets.

High rapidity cut